Università degli Studi di Bologna

FACOLTA' DI INGEGNERIA

Corso di Dottorato in
ING-IND/13: MECCANICA APPLICATA ALLE MACCHINE
Ciclo XX

A new approach for the dynamic modelling of the human knee

Tesi di Dottorato di:
Ing. Nicola Sancisi

Coordinatore:
Chiar.mo Prof. Vincenzo Parenti Castelli

Tutore:
Chiar.mo Prof. Vincenzo Parenti Castelli

Anno Accademico 2007-2008

Contents

Chapter 1

Introduction

The study and the analysis of the human knee is a particular sector of Orthopaedics which has constantly attracted the attention of researchers. The huge number of surgical operations which every year are devoted to total or partial articular replacements is an index of the importance acquired within the scientific community. Thus, it is not surprising that the growing attention on this field of research has recently exceeded the bounds of Orthopaedics and involved those of Physics, Mathematics and Engineering.

Great attention has been devoted in particular to the modelling of the knee. Models which can accurately reproduce certain characteristics of this joint are important tools which help to understand or to discern many functional aspects that could be difficult to observe by means of standard experimental analyses. The forces exerted by the muscles and by the other articular components of the knee are a clear example of the difficulties which can be found within the practice: the experimental procedures and tools which are now available to measure these forces are highly invasive and do not make it possible to obtain the required information. Nevertheless, the knowledge of the knee articular forces could be a support for clinical diagnoses and analyses; furthermore it could provide significant insights on the field of prostheses and orthoses [6].

As regards this point, knee models prove useful also as effective tools for the aided design of innovative prostheses and orthoses. This is not only the result of the amount of information which can be obtained easily and quickly from a model. As in other applications, knee models make it possible indeed to reduce the cost of the prototyping stage, since they allow designers to foresee the behaviour of a prosthesis or an orthosis once it has been implanted on a patient. Moreover, the use of models during the design stage would reduce the number of experimental tests which should be carried out *in vivo* or *in vitro* to optimize a particular design or to fit the patient characteristics.

Knee models also are fundamental instruments in the surgical planning of an operation or during the operation itself. Some models are used jointly with medical devices to customize or to modify prostheses and orthoses on an individual patient.

Furthermore, as in prosthesis design, knee models allow surgeons to foresee the behaviour of a prosthetic knee, in particular when the original articular components are modified or removed at all. Finally, the use of efficient models could reduce the experimental tests on the patient and the post-operation interventions.

Many models have been presented in the literature as a confirmation of their scientific and practical relevance [16]. Starting from the early bi-dimensional models [8, 21, 27, 35] and arriving at the recent three-dimensional ones [5, 15, 17, 19, 31, 37, 38, 45], the accuracy of the mechanical description of this articulation has constantly grown. In some cases these models have been defined from average data taken from the literature, otherwise they have been based on experimental data, trying to fit a particular required task.

In the last few years, many models have been proposed for the dynamic modelling of the knee joint [6, 16]. Their common target is to replicate the relative motion of the three main bones of the knee (i.e. the tibia, femur and patella) when a known set of forces are applied to the joint. Sometime the forces are time-dependant: this is the typical situation studied by the authors which model the motion of the knee during specific but significant tasks, such as during normal walking or rising movements [30, 31, 35, 41, 42]. Other studies examine the behaviour of the knee when static or quasi-static forces are applied, to obtain the equilibrium configurations of the joint [2, 4, 15, 17, 23, 26].

The final objective of all these studies is to define a model that fit a particular task. Many strategies have been devised to reach the target, but a common procedure could be outlined. This is what could be called a *simultaneous approach*: starting from a set of data obtained from the literature or from an experimental session, some elements of the knee are modelled, others are ignored; the parameters which define the knee model as a whole are identified in order to fit experimental results or medium values reported in the literature. The main differences between the models lie in the number of considered elements, in the model of each element and in the optimization approach used to fit the experimental results.

The simultaneous approach makes it possible to obtain models which can accurately replicate the relative motion of the tibia, femur and patella for a specific task. Unfortunately, the specificity of the task respect to which the models are identified represents also the main drawback and the fundamental limitation of this approach. The optimization of all parameters with no particular distinction among them makes sure that the functional and stabilising role of each structure of the knee is somehow lost. In other words, the basic function of each structure is not replicated in general in the model. As a result, the optimized model can simulate the knee motion during a given task, but nothing can be said *a priori* when other tasks are prescribed, or when the loading conditions of the joint are altered.

The main consequence of this drawback is that if these models can be useful and reliable to obtain data which could not be recorded in an experimental session (such as muscular or other articular forces), at the same time they present strict limitations for the planning of an operation or for the prosthetic design. These applications indeed have no fixed tasks; moreover, they require models which allow one to foresee the behaviour of the joint when the original conditions are modified.

The aim of this dissertation is to propose a novel approach for the dynamic modelling of the knee. The proposed procedure is directed to overcome the problems and limitations connected with the simultaneous approach. The dynamic model of the knee is defined gradually, by passing through a sequence of steps, i.e. of intermediate models, which allow the anatomical function of each structure of the joint to be correctly replicated. In particular, the procedure makes it possible to assign each articular component its correct role which, as a consequence, can be easily identified. The fundamental rules of the novel approach make sure the stabilizing role of these structures is preserved step after step, until the final model of the joint is obtained. The target of the new approach is to define models which can be useful and reliable also for those applications, such as the surgical planning and the prosthetic design, which cannot rely on specific tasks in general.

In order to prove the potentialities of the method, the new approach is exploited to define a stiffness model of the knee. This model can replicate the behaviour of the joint when external quasi-static forces are applied. The point of originality of the model lies on its gradual definition: a purely kinematic model is defined at first, in order to replicate the natural motion of the knee when no loads are applied to the joint; this model is then enriched with new elements which make it possible to extend the application of the model to quasi-static loading conditions.

The new approach and the theoretical and anatomical foundations of the model are presented in chapter 2. In order to show the accuracy of the model and the efficiency of the proposed procedure, the model is synthesized from experimental data in chapter 3 and the results are compared with those obtained both during an experimental session and with data published in the literature.

Chapter 2

The modelling of the human knee

The new approach and the theoretical and anatomical foundations of the knee model defined in this dissertation are presented in this chapter. A brief anatomical section introduces the main matter; the most important aspects of the proposed procedure are then described in section 2.2; finally, in sections 2.3 and 2.4 it is shown how to apply the procedure for the modelling of the human knee.

2.1 Anatomy of the knee

This section gives some basic information about the knee. Its scope is to describe the anatomical structures that are considered in the following. Furthermore, the nomenclature and the conventions adopted in this dissertation are presented. This paragraph is not meant to be a complete treatise about the human knee, but a short and simple reference to clarify those points which are used in this dissertation.

2.1.1 The knee components

The knee is a joint which allows the relative motion between three bones of the leg, i.e. the *tibia, femur* and *patella* (Figure 2.1). A forth bone, i.e. the *fibula*, is connected to the tibia by a strong but not rigid connection; anyway, the relative movements between the tibia and fibula will be ignored in this dissertation, since they are irrelevant as it will be clear in what follows. Two sub-joints could be recognized: the *tibio-femoral* (TF) and the *patello-femoral* (PF) joints, whose names come from those of the bones which enter into mutual contact during knee motion. As regards TF, two tibia proximal surfaces (i.e. the *tibial condyles*) move on two femur distal surfaces (i.e. the *femoral condyles*). As regards PF, the patella can slide on the femoral condyles and on the *trochlea*, i.e. the antero-distal surface of the femur between the condyles. The contacts between the femur and tibia actually are partly mediated by two cartilaginous elements, i.e. the *menisci*. The menisci are not considered in the model described in this dissertation; anyway, this simplification does not constitute a limitation of the proposed procedure.

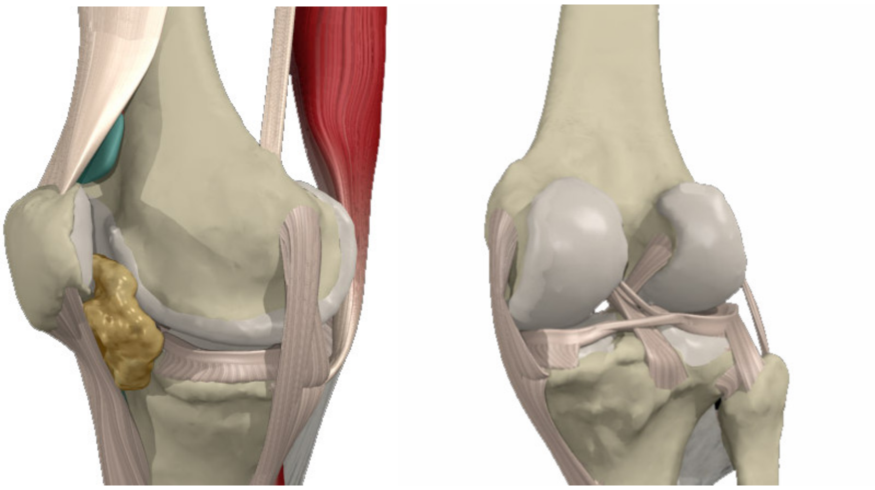

(a) Lateral view. (b) Back view.

Figure 2.1: A lateral view (a) and back view (b) of the knee. The main structures which constitute the joint are represented [34].

The knee is formed by several anatomical parts which will be called *structures*, *elements* or *components* in the following, without distinction. They can be divided into passive and active structures. Passive structures are those elements which can exert forces only if externally stressed: articular surfaces, menisci, ligaments and other ligamentous structures belong to this category. On the contrary, active structures — such as the muscles — can intrinsically exert forces but, in general, they almost do not oppose external forces when inactive.

Articular surfaces are those parts of the bones which enter into mutual contact during knee motion. In this case, they are the tibial and femoral condyles, the trochlea and the dorsal (or back) surface of the patella. Since the femoral condyles are two distinct surfaces, sometime they will be called the medial and lateral condyle; the same remark holds for the tibial condyles as well.

Ligaments are very important knee elements which have a strong influence on the stability of the joint. They are composed by a fibrous connective tissue; that is why when only a part of the ligament is considered, it is referred to as a fibre or a bundle of fibres. The most important ligaments of the knee provide a bone-to-bone interconnection between the tibia, fibula, femur and patella. The connective area between a ligament and a bone will be called *attachment* or *attachment area* in the following, without distinction. Thus, the two attachments of a certain ligament could be called the femoral and tibial attachments, for instance.

The four major ligaments which interconnect the tibia-fibula complex and the femur are the *anterior cruciate* (ACL), the *posterior cruciate* (PCL), the *medial collateral* (MCL) and the *lateral collateral* (LCL) ligaments; the patella is connected to the tibia by means of the *patellar ligament* (PL). Photographic images of these ligaments are presented in Figure 2.2: they were taken from a specimen,

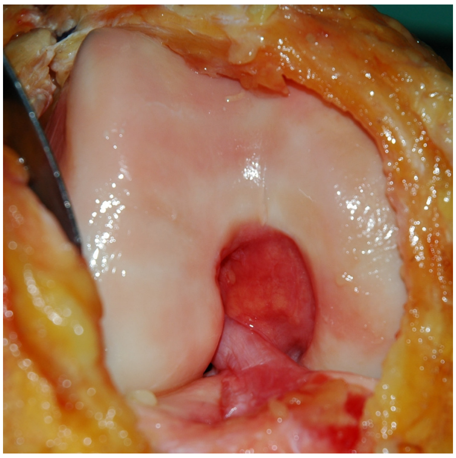

(a) The cruciate ligaments.

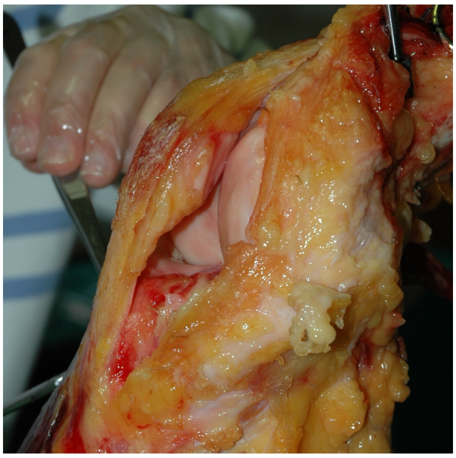

(b) The patellar ligament.

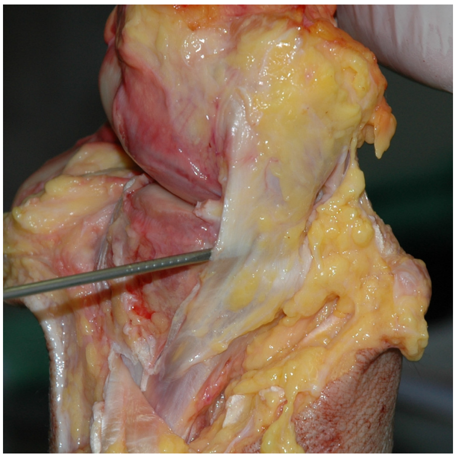

(c) The medial collateral ligament.

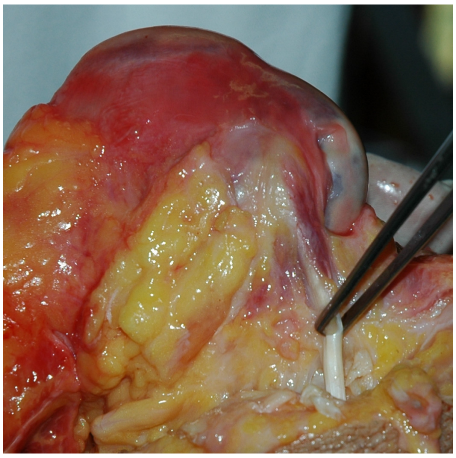

(d) The lateral collateral ligament.

Figure 2.2: The principal ligaments of the knee joint.

during an experimental section carried out at the Movement Analysis Laboratory of the Istituti Ortopedici Rizzoli (IOR) (section 3.1). Other ligaments considered in this dissertation constitute the so-called *posterior structures* of the knee, since they interconnect the posterior part of the tibia-fibula complex and that of the femur. They are the *arcuate ligament*, the *popliteus tendon* and the *oblique popliteus ligament*. Even if the popliteus tendon is not technically a ligament, it can exert passive forces due to its particular connection to the bones [43].

Knee muscles are not modelled in this dissertation, but only the quadriceps is presented here. It is the main muscle of the knee and it is made up of four distinct portions. All of them are attached to the patella on one side by means of the patellar tendon; on the other side, some portions are attached to the femur, while the others to the ilium.

2.1.2 The description of the knee motion

In order to identify every point of the joint, it is necessary to define reference frames. In particular, it is convenient to define three anatomical frames attached to the tibia, femur and patella respectively: the coordinates of a point of a bone expressed in the corresponding anatomical frame do not change with knee configuration. Moreover, the relative pose (position and orientation) between two bones can be described by means of the kinematic parameters which define the relative poses of the corresponding reference frames. Since the fibula is considered as rigidly attached to the tibia, these two bones share the same anatomical frame.

The three anatomical frame are represented in Figure 2.3. The tibia anatomical frame ($\mathscr{S}_t$) is defined with origin coincident with the tibia centre (on the tibial plateau); x-axis orthogonal to the plane defined by the two malleoli and the tibia centre, anteriorly directed; y-axis directed from the mid-point between the malleoli to the tibia centre; z-axis as a consequence, according to the right hand rule. The femur anatomical frame ($\mathscr{S}_f$) is defined with origin coincident with the mid-point between the lateral and medial epicondyles; x-axis orthogonal to the plane defined by the two epicondyles and the head of femur, anteriorly directed; y-axis directed from the origin to the head of femur; z-axis as a consequence, according to the right hand rule. Likewise, the patella anatomical frame ($\mathscr{S}_p$) is defined with origin coincident with the mid-point between the lateral and medial apices; x-axis orthogonal to the plane defined by the lateral, medial and distal apices, anteriorly directed; y-axis directed from the distal apex to the origin; z-axis as a consequence, according to the right hand rule.

A relative pose of the femur with respect to the tibia can be expressed by means

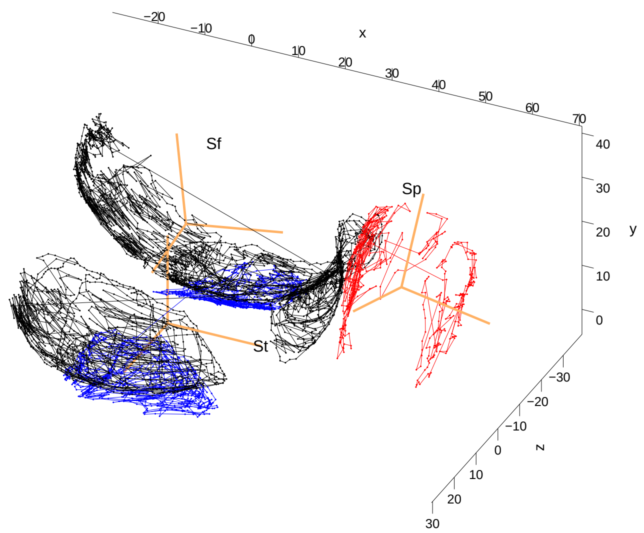

Figure 2.3: The three anatomical frames $\mathscr{S}_t$, $\mathscr{S}_f$ and $\mathscr{S}_p$ (orange) represented together with the tibial (blue), femoral (black) and patellar (red) articular surfaces.

of the position $\mathbf{P}_{tf}$ of the origin of $\mathscr{S}_f$ in $\mathscr{S}_t$, and by means of the 3x3 rotation matrix R_{tf} for the transformation of vector components from $\mathscr{S}_f$ to $\mathscr{S}_t$. Matrix R_{tf} can be expressed as a function of three rotation parameters α, β and γ:

$$R_{tf} = \begin{bmatrix} c_\alpha c_\gamma + s_\alpha s_\beta s_\gamma & -s_\alpha c_\gamma + c_\alpha s_\beta s_\gamma & -c_\beta s_\gamma \\ s_\alpha c_\beta & c_\alpha c_\beta & s_\beta \\ c_\alpha s_\gamma - s_\alpha s_\beta c_\gamma & -s_\alpha s_\gamma - c_\alpha s_\beta c_\gamma & c_\beta c_\gamma \end{bmatrix} \tag{2.1}$$

where c and s indicate the cosine and sine of the angle in subscript and α, β, γ represent the flexion, ab/adduction and intra/extra rotation angles of the femur relatively to the tibia, using a convention deduced by the Grood and Suntay joint coordinate system [13]. According to this convention, flexion is a rotation about the z-axis of $\mathscr{S}_f$, intra/extra is a rotation about the y-axis of $\mathscr{S}_t$, ab/adduction is a rotation about a floating axis, perpendicular to the previous ones. Positive signs of α, β and γ correspond respectively to femoral flexion, adduction and external rotations. Expression (2.1) can be applied for right legs; in order to use the same matrix for left legs, the signs of β and γ should be inverted in (2.1). Likewise, the matrix R_{fp} and the vector $\mathbf{P}_{fp}$ express a relative pose of the patella with respect to the femur; the matrix R_{fp} can be represented by an expression similar to (2.1). Even though the Grood and Suntay convention was originally defined for the tibio-femoral joint, its application on different joints (the patello-femoral joint included) is becoming ordinary in the scientific literature.

2.2 A novel procedure for the knee modelling

2.2.1 The sequential approach

The main limitations of the simultaneous approach applied to the knee modelling have been presented in chapter 1. The simultaneous identification of all the model parameters does not guarantee that the functional and stabilising role of the articular structures is correctly replicated within the model. As a consequence, the optimized model can simulate the knee motion during a given task, but if the loading conditions are changed the model could not be reliable any more. This drawback limits the use of the model for applications which have no fixed tasks and which require models to foresee the behaviour of the knee when the original conditions are modified.

It is clear that the perfect solution would be the definition of a model which could be accurate and reliable for every loading conditions. This is probably a dream at the moment, but the simultaneous approach does not seem the proper procedure to try to reach this target, for all the reasons which have been pointed out. On the contrary, it could be more promising to start building the model from its foundations, trying to fit as best as possible simple but basic tasks. These basic tasks are particular loading conditions which emphasize the restraining role of certain elements of the knee; they should be simple since they should show the

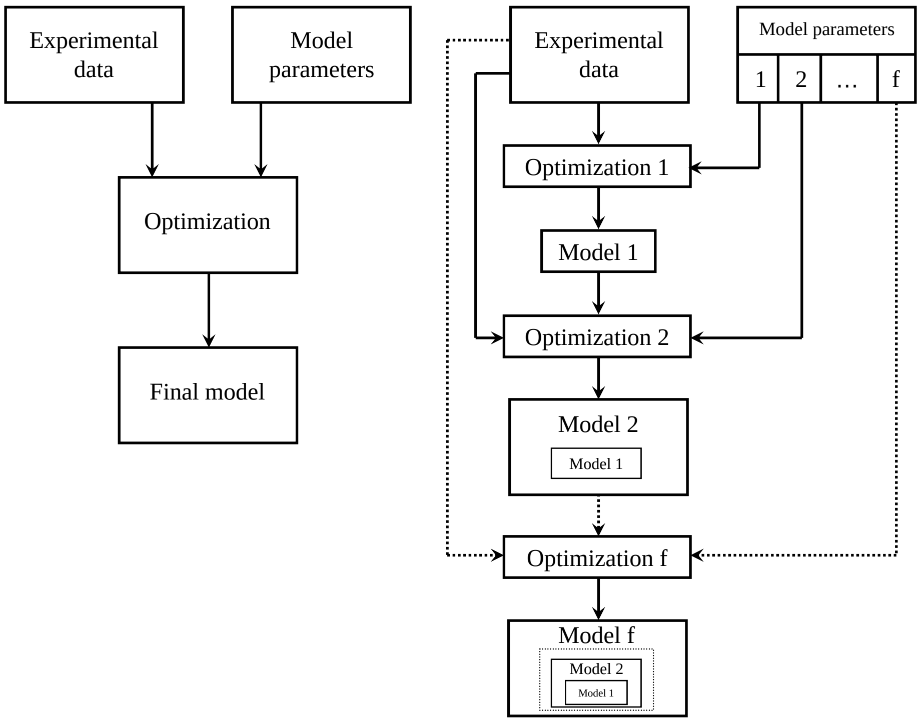

(a) The simultaneous approach. (b) The sequential approach.

Figure 2.4: Comparison between the simultaneous (a) and the sequential approach (b).

stabilizing role of a limited number of structures at a time, making it possible to recognize those parameters that do not influence a certain behaviour of the joint. In this sense these tasks are an important foundation of the model and thus they should be used as a reference: they make it possible to model only those structures at a time which guide a particular basic motion of the knee.

The articular components are sequentially added to the model, in order to fit more and more complex tasks: the model grows from its foundations and the stabilizing roles of each element of the joint is emphasized. Moreover, the model becomes more and more sophisticated, making it possible to replicate the motion of the knee even under complex loading conditions. In order to make sure the function of each structure is preserved, it is fundamental that the addition of new elements does not interfere with the motion of the knee during previous simpler tasks. This is the most important condition to guarantee that, when the knee is subjected to the loading conditions of a basic task, only determinate elements could affect the joint motion.

This particular procedure will be called *sequential approach* in this dissertation, in contrast with the simultaneous approach described before. A comparison between the two procedures is shown in Figure 2.4. While in the simultaneous approach the knee model is defined by means of one large-scale optimization only — preceded or followed by few small adjustments to the model parameters —, in the sequential approach the model is defined by means of a sequence of partial optimizations which lead to a more and more sophisticated model, till the *final* one is obtained. In a certain sense, the final model is built starting from a basic block; other blocks are then added, until the final building is completed.

From an operative point of view, the sequential approach makes it possible to identify the model parameters by means of a number of sequential steps. At each step only some parameters are identified, satisfying fundamental anatomical constraints and characteristics of the knee.

The procedure is based on two important rules to achieve this objective:

1. Once a parameter has been identified at a particular step, it is not changed at the following steps;

2. Parameters identified at each step must be chosen so that they do not alter the results obtained at the previous steps.

These two rules guarantee that the results obtained at each step do not worsen those already obtained at previous steps and, most importantly, they make it possible to choose new parameters of the model respecting the anatomical constraints satisfied at previous steps. The stabilizing role of the knee elements is so preserved, as new elements are added at each step.

In this sense, the proposed sequential approach is substantially an inductive procedure which starts from the definition of a simple model which can replicate the behaviour of the joint under very strict loading conditions. This preliminary model is then enriched, i.e. made more sophisticated, at each step, in order to obtain a more and more generalized model which can replicate the behaviour of the knee under more and more generic and complex loading conditions.

2.2.2 The passive motion of the knee

The sequential approach is only a partial aspect of the novel procedure which is proposed in this dissertation for the modelling of the human knee. It is indeed evident that the sequential approach needs a starting point, i.e. a preliminary model which can satisfy a first basic task and which represents the foundation of the final model. Being the first block of the procedure, the choice of the first basic task and its modelling are both crucial points for the complete knee model.

It is proposed here to choose the passive motion of the knee as a starting point of the sequential approach. The passive motion of the knee is the relative motion of the tibia, femur and patella when no loads (external or muscular) are applied to the joint. Experience shows that when no loads are applied to the knee, the joint does not have a single, well defined equilibrium position; on the contrary, the knee can assume an infinite number of possible configurations, all connected together.

This mobility is exactly the passive motion of the knee, i.e. the unresisted motion of the joint [10, 27, 45].

In a certain sense, the particular loading condition of the passive motion is the simplest one which can be exerted on the knee: this aspect meets the basic task requirement of *simplicity* and makes the passive motion a good candidate as a starting point for the sequential approach. This, however, is not the only reason which leads to choose the passive motion as the first step of the proposed procedure. Several studies [10] prove that knee stability is directly connected to the passive motion of the joint. As a direct consequence, a full understanding of this motion can provide significant insights on the role of the passive elements of the knee in the achievement of the joint stability. This is an important task for knee restoration and prosthetic design.

The passive motion is thus chosen as the first step of the sequential approach. The preliminary model of the knee — i.e. the result of the first step of the sequential approach — replicates the passive motion only and includes only the articular elements which affect this particular motion. Only model parameters associated to these elements are identified. It is thus important to discern which structures influence the passive motion, in order to exclude the others; moreover it is fundamental to define an accurate and efficient preliminary model in order to provide the final model a good foundation.

2.2.3 The *in vivo* feasibility of the basic tasks

A further principle should be considered in the choice of basic tasks. The models which stem from each step of the sequential approach are defined by means of a number of parameters which have to be identified on experimental data. These data could be obtained from the literature or from a knee *in vivo* or *in vitro*.

Several authors (see, for instance, [24]) proposed procedures that make it possible to model the knee or its structures by means of invasive experimental techniques. Those include cutting and separation of bone segments, dislocation of articular components, exsection of ligaments or other elements of the joint. These techniques are often a requirement in order to acquire the experimental data which are needed for the parameter identification of the models.

Invasive techniques allow researchers to obtain experimental data which could be very difficult — if not impossible — to acquire otherwise; therefore they are an important source for many research purposes. As regards knee modelling, invasive techniques are thus useful to define and identify models for research and theoretical applications. On the contrary, it is clear that invasive techniques cannot be used when the model has to be defined for surgical planning or prosthetic design. These applications indeed need data which have to be obtained *in vivo* and, as a consequence, they have to be acquired by means of experimental techniques as less invasive as possible.

The choice of the basic tasks should take this aspects into proper consideration: if the model has to be used for practical purposes, it must be possible to replicate the basic tasks *in vivo* by means of non-invasive techniques. If this principle is satisfied, it is actually possible to identify the model on the experimental data recorded from a patient.

The procedure proposed in this dissertation makes use of basic tasks which satisfy this principle. As explained in section 3.1, it was impossible to carry out an experimental session *in vivo* due to technical limitations, and the experimental data were recorded from a specimen or taken from the literature. Anyway, having the opportunity, the same data could have been obtained by means of non-invasive techniques also. It should be stressed, for instance, that the passive motion of the knee could be obtained *in vivo*.

Section 2.2 presented the main aspects of the novel approach which is used in this dissertation to model the knee joint. The application of the proposed procedure is presented in next sections; in particular, it is shown how to apply the procedure in order to obtain a stiffness model of the knee, starting from a passive motion model. Moreover, some details are provided on how to apply the procedure in order to further generalize the knee model.

2.3 First step: the model of the passive motion

Several studies [10, 45] prove that the relative movement of the tibia and femur during passive flexion is a one degree of freedom (dof) motion: once the flexion angle is imposed to the articulation, the corresponding pose of the tibia with respect to the femur is defined, both univocally and experimentally replicable. The same result holds also for the relative movement of the patella and femur [1]: despite the patello-femoral joint (PF) is slightly more slack during passive flexion if compared to the tibio-femoral joint (TF), experimental results prove that for a given flexion angle of the knee the relative pose of the patella with respect to the femur is replicable. As a consequence, the patella also shows a one dof of unresisted motion with respect to the femur.

Most papers dealing with 2D [35] and mainly 3D [5, 15, 16] modelling of the knee joint in passive motion consider more or less complex models which comprise visco-elastic connections between the involved structures. These models may be interesting but are computationally expensive. Moreover the identification of the anatomical parameters (stiffness, viscosity,...) may be critical.

A further and more important point leads to the conclusion that these models do not fit well with the proposed sequential approach. The point stems from the equilibrium analysis of the joint under unloaded conditions. Since no forces are exerted on the articulation, no forces can be exerted by the passive structures of the knee to satisfy the equilibrium of the system composed by the tibia, femur and patella. The internal forces due to the passive structures could be internally auto-balanced, thus invalidating the concept of totally unloaded condition, but these circumstances would be extremely complex to achieve on the full flexion-extension movement, even considering friction between articular components. As a consequence, the ligaments and in general the passive structures of the knee cannot be tight during passive flexion: they can reach the limit between laxity and tension at the most.

All these observations involve important anatomical constraints which must be considered and satisfied by the knee model: when no forces are applied to the model of the knee, the relative motion of the tibia, femur and patella must be a one dof motion and the passive structures of the knee must not be tight. The most important consequence is that visco-elastic properties have no influence on the passive motion of the knee; moreover there are some components of the joint which do not even guide the passive motion, since they cannot exert forces being lax. These components can thus be ignored in the model of the passive motion: as explained in section 2.2.2, this model must include only the elements that affect this motion, and only the parameters which have an influence can be identified. This is a fundamental aspect of the sequential approach and this is why the models proposed in the cited studies cannot be used with the proposed procedure. Thus, a different approach should be followed for the modelling of the passive motion.

This approach stems from static-kinematic considerations [27]. Since knee flexion is guided along a one dof motion despite all its structures are slack or at the limit between tension and laxity, there exist some articular components which persist in this last status during the complete passive flexion: these structures are those which guide and that affect the passive motion. Furthermore, since no forces are applied to these components, they are subjected to no deformations. The fundamental conclusion is that the passive motion of the knee can be modelled by means of a rigid link mechanism; the relative motion of the tibia, femur and patella can thus be obtained from the kinematic analysis of the *equivalent mechanism*.

The idea of equivalent mechanisms is not new and could be dated back to the classic four-bar mechanism (Figure 2.5(a)) [21]. Anyway the first three-dimen-

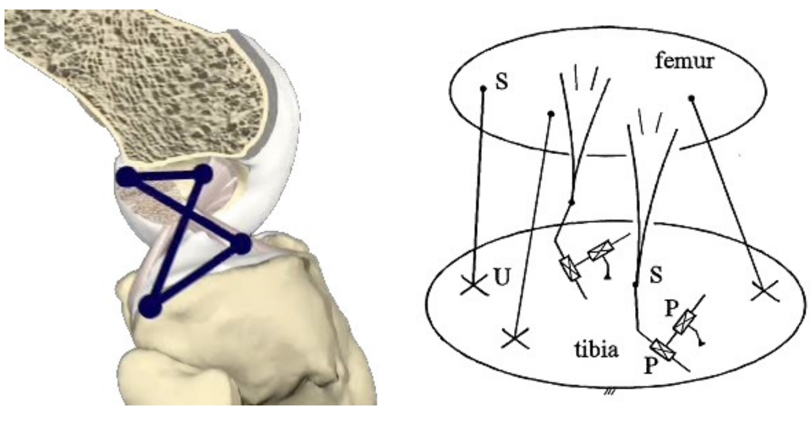

(a) The four-bar linkage.

(b) A recent 3D model.

Figure 2.5: Two equivalent mechanisms of the tibio-femoral joint: the classic four-bar linkage [21] (a) and a recent 3D model [45] (b).

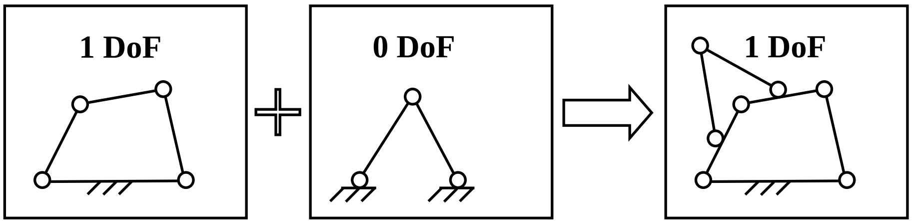

Figure 2.6: The two sub-chains of the passive motion model.

sional (3D) mechanisms which can replicate the motion of TF [45] (Figure 2.5(b)) appeared only recently in the literature. The first 3D equivalent mechanism which replicates the passive motion of the *total* knee (PF included) was recently presented in [38]. The main reason that led other authors to ignore the PF joint in the first 3D models is the partial independence of the TF motion with respect to the PF one: the passive motion of TF is independent from that of PF if tibia flexion is imposed. Thus the two sub-joints of the knee can be analysed separately and, in particular, TF can be modelled without taking PF into consideration.

The explanation of this aspect relies on the anatomical constraints between the two sub-joints. As explained in section 2.1, the patella slides on the femoral distal surfaces while it is connected to the tibia through the patellar ligament, and to the femur through the quadriceps. This muscle does not exert any forces on the patella during passive motion; moreover, the slight laxity of the quadriceps and the particular conformation of the joint make sure PF does not constitute a constraint to TF in this case. In other words, the patella moves on the femur surfaces being trailed by the patellar ligament.

It is important to note that, in order to respect the anatomical behaviour of the joint, the independence of the motion of TF from that of PF is not only an advantage, since it makes it possible to define the model of TF independently from that of PF, but incidentally it is also a requirement of the model of the complete joint. The knee model must show the same feature, to make sure it correctly replicates the anatomical constraints of the joint. As a consequence, the equivalent mechanism of the knee passive motion has to be composed by two sub-chains, i.e. two partial mechanisms, which show the requirement of partial decoupling. The first sub-chain is the model of TF and it must have one dof. The second sub-chain is the model of PF: it is connected to the previous one and it must have zero dofs. The complete mechanism exhibits one dof and the motion of the TF sub-chain is independent from that of the PF sub-chain if knee flexion is imposed. The Figure 2.6 clarifies this concept with planar mechanisms. The addition of a sub-chain with mobility zero to a mechanism does not change the mobility of the whole mechanism.

The two parts of the equivalent mechanism of the knee passive motion are presented separately in the following sections.

2.3.1 The model of the tibio-femoral joint

In the last few years, several mechanisms were presented which can accurately replicate the passive motion of TF by means of three-dimensional rigid link mechanisms. Starting from the first one [45], a group of models was proposed which showed an increasing complexity [19, 33, 32, 28].

The geometric and kinematic observations which support these mechanisms are almost the same. Experimental analyses show that a bundle of fibres of the ACL, one of the PCL and another of MCL remain almost isometric during passive flexion. These bundles are called *isometric fibres* (IF). The other bundles of these ligaments are slack and reach the limit between tension and laxity at the most. Articular contact is preserved during passive motion: the medial and lateral femoral condyles enter into contact with the corresponding tibial condyles on two points (one for the medial and the other for the lateral compartments). All the other components of TF are slack and do not constrain the passive motion. As a consequence, the three IF and the two pairs of condyles are the only anatomical structures which guide and affect the passive motion of TF [44]. If the isometric fibres are assumed as truly isometric and the contacts are assumed to occur on two points, a 3D parallel mechanism can be defined (Figure 2.7). This mechanism features two rigid bodies t and f (representing the tibia and femur) interconnected by three rigid binary links $\mathbf{A}_1\mathbf{B}_1$, $\mathbf{A}_2\mathbf{B}_2$, $\mathbf{A}_3\mathbf{B}_3$ (representing the three IF); each link is connected to both rigid bodies by means of spherical pairs. Moreover, two surfaces attached to the first rigid body τ_1 and τ_2 (representing the tibial condyles) remain in contact with two surfaces σ_1 and σ_2 (representing the femoral condyles) attached to the second rigid body. If the rotations of each binary link about its own axis are ignored, this mechanism shows one dof: the five constraints (the three links and

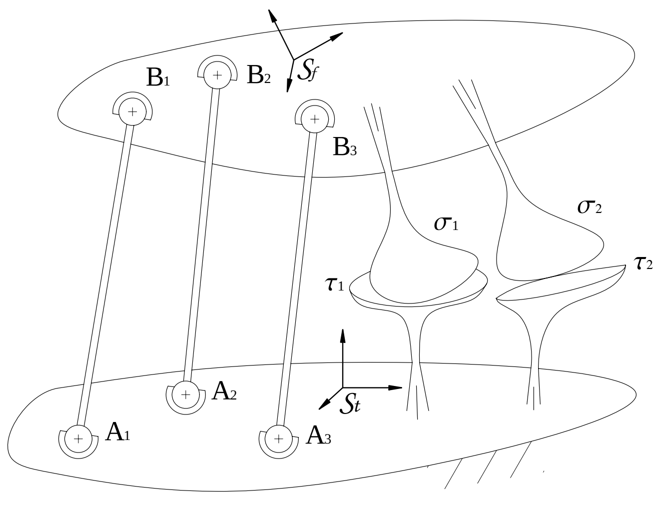

Figure 2.7: The generic 3D parallel mechanism for the modelling of the TF passive motion.

the two contacts) remove one dof each from the relative motion of the two rigid bodies. Mobility and a synthesis procedure of this type of mechanisms have been investigated in [22].

The approximation of the model consists both of substituting the three ligaments with the almost isometric fibres of the corresponding ligaments and of assuming these fibres as truly isometric. Furthermore the condyles are approximated by lower-order surfaces that (two by two) move on each other, entering into contact on a single point per surface. The main difference among the models cited above is an even more accurate representation of the articular surfaces, while the concept of isometric fibres remains the same.

The increasing complexity of these models leads to a greater complexity of the corresponding mathematical models which define the kinematic analysis of the equivalent mechanisms. The kinematic analysis is the fundamental tool which makes it possible to obtain the relative motion of the tibia and femur by means of the equivalent mechanisms, as described in the introductory part of this section. In order to simplify computations, a further mechanism was recently presented that replicates the passive motion of the knee with a similar accuracy than the previous models, even if, reversing the common tendency, it is considerably simpler than the others [37]. This was possible by exploiting other kinematic properties of TF, with respect to the previous models. This model was proposed as a support for prosthetic design and for operation planning, in particular, since it allows faster and more stable computations, at the same time producing a mechanically simple solution.

A further reason which suggests to use models with a suitable complexity is that accuracy does not increase with complexity all the time. Numerical instabilities may arise indeed from the kinematic analysis of a too complex mechanism and the number of parameters of the model makes the identification from experimental results very difficult and time-expensive. The limitations of higher-order models were shown in [28]. The substitution of lower-order surfaces with more complex ones did not produce particular benefits; on the contrary, the use of b-splines brought computational and optimization instabilities and the high order of the problem generated oscillations which, paradoxically, gave worse results than those of simpler models.

In a recent investigation carried out in [29], the approximation of the articular surfaces with spheres [33] proved very efficient for the modelling of the TF passive motion in analytical applications, providing a good balance between complexity of the model and accuracy of the synthesized motion. Thus, the same approximation is adopted in this dissertation also. It is worth noting that this model is kinematically equivalent to a one dof 5-5 parallel mechanism, which features two rigid bodies interconnected to each other by 5 binary links, through spherical joints (Figure 2.8). The centres of the spherical surfaces on the femur are forced indeed to remain at the same distance from the corresponding centres of the spherical surfaces on the tibia: the condyles can be substituted by two rigid binary links (similar to those representing the three IF) which connect two by two the centres of these

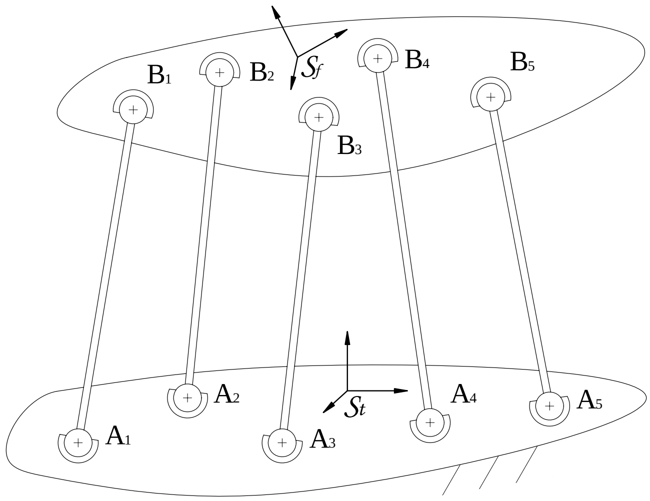

Figure 2.8: The 5-5 parallel mechanism.

spheres. In conclusion, three out of the five rigid links represent the isometric fibres of ACL, PCL and MCL, while the other two — hereafter called as contact fibres (CF) — substitute the articular contacts between the medial and lateral condyles of the tibia and femur.

In order to obtain the passive motion of TF, the relative poses of the femur with respect to the tibia have to be obtained from the model for each prescribed flexion angle. Each pose can be expressed by means of the matrix R_{tf} and the vector $\mathbf{P}_{tf}$: the first is the 3x3 rotation matrix for the transformation of vector components from $\mathscr{S}_f$ to $\mathscr{S}_t$; the second is the position vector of the origin of $\mathscr{S}_f$ in $\mathscr{S}_t$. Matrix R_{tf} can be expressed as a function of three rotation parameters α, β and γ, as reported in equation (2.1). The required poses can be obtained by solving the closure equations of the 5-5 mechanism representing TF. As previously noted, these equations can be solved independently from those of the PF sub-chain since the relative motion of TF is not influenced by that of PF in passive flexion. The closure equations of the mechanism constrain each pair of points $\mathbf{A}_i\mathbf{B}_i$ to keep the same distance at each imposed flexion angle:

$$\left\| \mathbf{A}_i - R_{tf}\mathbf{B}_i - \mathbf{P}_{tf} \right\| = L_{0i}, \quad (i = 1, \dots, 5) \tag{2.2}$$

where points $\mathbf{A}_i$ and $\mathbf{B}_i$ are the centres of spherical pairs, expressed in $\mathscr{S}_t$ and in $\mathscr{S}_f$ respectively (Figure 2.8) and L_{0i} are the lengths of links $\mathbf{A}_i\mathbf{B}_i$; $\|\cdot\|$ is the $\mathscr{L}^2$-norm of the vector. If the flexion angle α is assigned, (2.2) is a system of five equations in the five unknowns β, γ and $\mathbf{P}_{tf}$ components, which can be solved, for instance, by means of a quasi-Newton numerical procedure. The solution defines the relative pose of the femur with respect to the tibia for a given flexion angle.

The coordinates of the points $\mathbf{A}_i$ in $\mathscr{S}_t$, those of the points $\mathbf{B}_i$ in $\mathscr{S}_f$ and the link lengths L_{0i} $(i = 1 \dots 5)$ constitute a set of 35 geometrical parameters which define the TF model. The first step of the sequential approach consists in identifying the parameters of the passive motion model from experimental data; the identification of the geometrical parameters which define the TF model is the first part of this step. The procedure of identification — based on optimization — and the experimental session are described in sections 3.1 and 3.2. The parameters that define the structures which guide the passive motion of TF are thus determined as a result of this preliminary identification procedure. These parameters are not changed during the following steps, in order to observe the first rule of the sequential approach.

2.3.2 The model of the patello-femoral joint

A common characteristic of all the three-dimensional rigid link mechanisms for the modelling of the passive motion of the knee is that the patella is never considered. This simplification stems from the observation that, in passive motion, PF has no influence on the relative motion of the femur and tibia, as explained in the introductory part of this section. On the contrary, as well known by experimental evidence and models presented in the literature [8, 17, 36], under different loading conditions the patella affects the TF motion during flexion: the stabilizing effect of PF on the loaded knee is a fundamental aspect of the joint mechanics which cannot be ignored. Thus, in order to define a passive model of the whole knee which can be used as a starting point for the sequential approach, the relative poses of the patella and femur must be known.

A few models which can replicate the passive motion of PF have been presented in the literature. Most of them consider deformations of the PF components and their visco-elastic properties [15]. The only rigid link mechanisms which have been proposed in the past for the modelling of PF are two-dimensional models of the relative motion of the femur and patella on the sagittal plane [8]. A 3D equivalent mechanism for the simulation of PF in passive motion has been presented in [38] only recently; in the same study, a 3D mechanism for the modelling of the passive motion of the whole knee has been proposed.

The equivalent mechanism of PF can be defined by means of anatomical and kinematical considerations about the relative motion of the patella and femur. The contact between the patella and femur occurs on a wide portion of their rigid articular surfaces for each flexion angle (Figure 2.9): this observation suggests that this contact can be modelled by means of a lower pair. In particular, the trochlea and the portions of femoral condyles which are involved in the contact can be approximated by a cylinder. Thus, the relative motion of the patella and femur occurs about a fixed relative axis, i.e. the axis of the approximating cylinder. Moreover, the particular shape of the articular surfaces ensure that the patella has a limited mobility along the rotation axis: the dorsal surface of the patella fits — in a certain sense — the trochlea, the femoral condyles and the intercondylar space. These considerations all lead to the conclusion that the contact between the patella and femur can be modelled by a hinge joint which mutually connects the two bones. Furthermore, experimental observations show that a bundle of fibres of the patellar

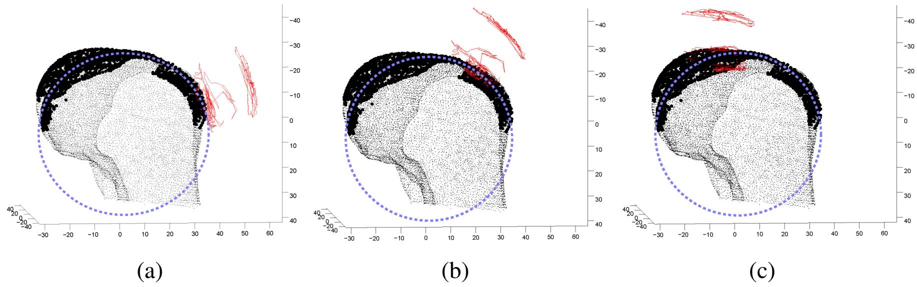

Figure 2.9: The articular contacts between the patella (red lines) and femur (black points) at three different flexion angles. The cylindrical approximation of the condyles (blue circle) is also presented.

ligament remains almost isometric in passive flexion. This is a direct consequence of the absence of articular forces. Thus, it is possible to substitute this bundle with a rigid link: this link connects the patella to the tibia, its endings joined to the bones by means of spherical pairs.

In order to obtain a complete kinematic model of the knee, it is necessary to set the parameter of the motion whose value determines the configuration of the joint. The flexion movement when imposed by the muscles can be seen as the result of the action (lengthening or shortening) of the quadriceps on the patella, which transmits the muscle forces to the tibia and femur by means of the patellar ligament and the articular contacts respectively. In other words, the length of quadriceps fixes the configuration of the joint: this can be accomplished in the model, by substituting the quadriceps with a link which connects the patella and femur by means of a spherical-prismatic-spherical pair. It is worth noting that the quadriceps is actually connected to both the femur and ilium, as reported in section 2.1.1; since the relative motion between the femur and ilium is not considered in this dissertation, these two bones can be seen as a single rigid body.

The models of PF and of the knee in passive flexion are represented in Figure 2.10. The equivalent mechanism of PF (Figure 2.10(a)) features a rigid body p (representing the patella) constrained to rotate about an axis $\mathbf{n}_1$ fixed to a second rigid body f (representing the femur). The member p is connected to a third rigid body t (representing the tibia) by means of a rigid link $\mathbf{C}_1\mathbf{D}_1$ (representing the patellar ligament), connected to f and p by means of spherical pairs. Finally, the group $\mathbf{C}_2\mathbf{D}_2$ — composed by two rigid binary links connected by a prismatic joint — fixes the distance between the centre $\mathbf{D}_2$ of the spherical joint on p and the centre $\mathbf{C}_2$ of the spherical joint on f, by means of the axial translation parameter s of the prismatic joint. It is true that in this model the patella moves on a plane attached to the femur; unlike [8], however, this plane does not correspond necessarily to the sagittal plane of the body, but it moves with the femur; furthermore, the patella is guided by the link $\mathbf{C}_1\mathbf{D}_1$ which does not necessarily lies on the same plane of the patella motion. As a consequence, the model of PF is actually a 3D equivalent mechanism.

The approximation of the model consists both of substituting the patellar ligament with its almost isometric fibre and of assuming this fibre as truly isometric. The greater simplification resides however in the approximation of the articular contacts. It has been chosen because the consequent PF model is simple, stable and makes it possible to obtain good results all the same.

The model of the whole knee can be obtained by joining the TF and PF equivalent mechanisms (Figure 2.10(b)). The linear displacement s of the prismatic joint defines the configuration of the knee when the flexion angle is imposed by the quadriceps. It can be proved indeed that the presented mechanism has one dof (ignoring idle inessential dofs): the PF sub-chain — i.e. the chain constituted by members $\mathbf{C}_1\mathbf{D}_1$, the group $\mathbf{C}_2\mathbf{D}_2$ and the patella — shows zero dofs with respect to the TF complex if the prismatic joints is idle; thus it does not reduce the number of dofs of the TF mechanism, i.e. one dof. This is compatible with the previous anatomical observations: PF does not constrain TF in passive conditions and, if the flexion angle is externally imposed, the motion of TF is independent from that of PF; on the contrary, the motion of PF is defined by TF. The movement which is obtained by leaving the prismatic pair idle reproduces the passive motion of the knee.

The motion of PF during passive flexion can be obtained from the model by computing the relative poses of the patella with respect to the femur for each prescribed flexion angle. As for TF, each pose can be expressed by means of the matrix R_{fp} and the vector $\mathbf{P}_{fp}$: the first is the 3x3 rotation matrix for the transformation of vector components from $\mathscr{S}_p$ to $\mathscr{S}_f$; the second is the position vector of

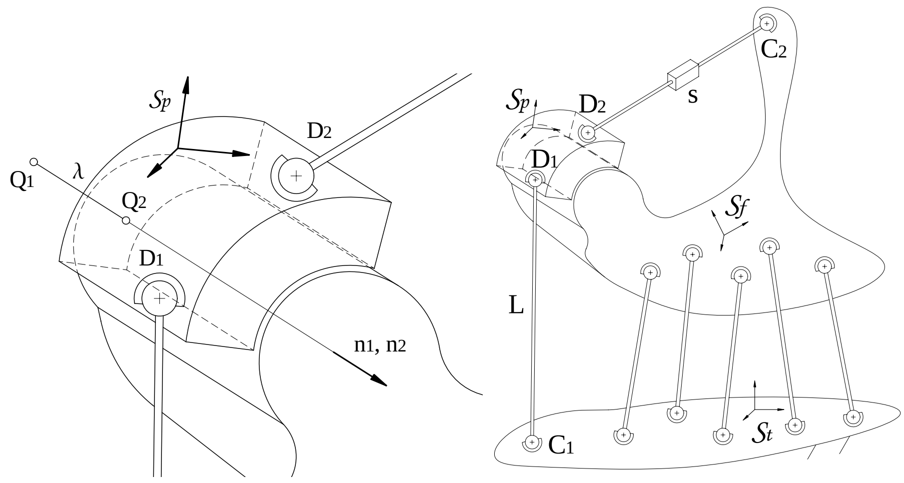

(a) The patello-femoral joint. (b) The complete knee model.

Figure 2.10: The kinematic model of the patello-femoral joint (a) and of the knee joint (b). In the figure, the geometrical parameters of the patello-femoral joint are also represented.

the origin of $\mathscr{S}_p$ in $\mathscr{S}_f$. Matrix R_{fp} can be expressed as a function of three rotation parameters α, β and γ, as reported in equation (2.1). As for the TF mechanism, the required poses expressed by R_{fp} and $\mathbf{P}_{fp}$ can be obtained by solving the closure equations of the PF sub-chain. These equations provide the connection between the geometrical parameters and the coordinates of the relative poses of the patella and femur.

The geometrical parameters involved in the PF model (Figure 2.10(a)) are the components of the unit vectors $\mathbf{n}_1$ and $\mathbf{n}_2$ of the hinge rotation axis expressed respectively in $\mathscr{S}_f$ and $\mathscr{S}_p$, the coordinates of the position vectors $\mathbf{Q}_1$ and $\mathbf{Q}_2$ of the intersections of the same axis with the x-y reference planes expressed respectively in $\mathscr{S}_f$ and $\mathscr{S}_p$, the coordinates of the insertion points $\mathbf{C}_1$ and $\mathbf{D}_1$ expressed respectively in $\mathscr{S}_t$ and $\mathscr{S}_p$, the fixed distance L between $\mathbf{C}_1$ and $\mathbf{D}_1$ and the fixed distance λ between $\mathbf{Q}_1$ and $\mathbf{Q}_2$. Since the norm of the hinge unit vector is unitary, the components of the unit vectors $\mathbf{n}_1$ and $\mathbf{n}_2$ can be expressed as a function of two independent coordinates only, for instance the azimuth δ and the altitude η, y-z being the horizontal plane and z-axis the azimuth origin (Figure 2.11):

$$\mathbf{n}_1 = \begin{pmatrix} \sin\eta_1 \\ \cos\eta_1 \sin\delta_1 \\ \cos\eta_1 \cos\delta_1 \end{pmatrix}, \quad \mathbf{n}_2 = \begin{pmatrix} \sin\eta_2 \\ \cos\eta_2 \sin\delta_2 \\ \cos\eta_2 \cos\delta_2 \end{pmatrix} \tag{2.3}$$

Furthermore, the coordinates of the position vectors $\mathbf{Q}_1$ and $\mathbf{Q}_2$ admit the following representation:

$$\mathbf{Q}_1 = \begin{pmatrix} x_1 \\ y_1 \\ 0 \end{pmatrix}, \quad \mathbf{Q}_2 = \begin{pmatrix} x_2 \\ y_2 \\ 0 \end{pmatrix} \tag{2.4}$$

From (2.3) and (2.4) and from the previous considerations, it follows that the PF model is described by means of 16 independent geometrical parameters. It is worth

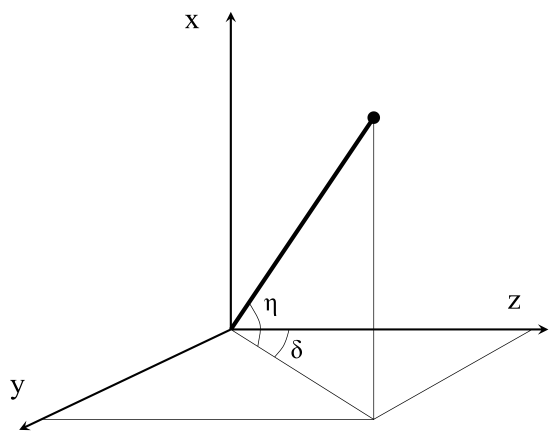

Figure 2.11: The azimuth δ and the altitude η angles which identify the $\mathbf{n}_1$ and $\mathbf{n}_2$ unit vectors with respect to $\mathscr{S}_f$ and $\mathscr{S}_p$.

noting that the parameters which define the position of points $\mathbf{C}_2$ and $\mathbf{D}_2$ are not taken into account since they are not necessary for the solution of the position analysis problem of the mechanism in passive flexion: since the prismatic joint is idle, the group $\mathbf{C}_2\mathbf{D}_2$ does not influence the motion of both the patella and femur.

The set of 16 parameters is used to define the closure equations of the PF model:

$$\begin{aligned} &R_{fp}\mathbf{n}_2 = \mathbf{n}_1 \\ &R_{fp}\mathbf{Q}_2 + \mathbf{P}_{fp} = \lambda \mathbf{n}_1 + \mathbf{Q}_1 \\ &\left\| R_{tf}\left(R_{fp}\mathbf{D}_1 + \mathbf{P}_{fp}\right) + \mathbf{P}_{tf} - \mathbf{C}_1 \right\| = L \end{aligned} \tag{2.5}$$

where $\|\cdot\|$ is the $\mathscr{L}^2$-norm of the vector. The first two vectorial equations force the axis identified by $\mathbf{n}_1$ and $\mathbf{Q}_1$ to be coincident with that identified by $\mathbf{n}_2$ and $\mathbf{Q}_2$. Moreover, the second vectorial equation imposes a constant distance between $\mathbf{Q}_1$ and $\mathbf{Q}_2$. The last scalar equation ensures that the distance between $\mathbf{C}_1$ and $\mathbf{D}_1$ is constant.

If the relative motion of the femur and tibia is given — i.e. if R_{tf} and $\mathbf{P}_{tf}$ are known by solving the closure equations (2.2) — (2.5) is a system of seven equations in six unknowns, i.e. the three components of $\mathbf{P}_{fp}$ and the angles α, β, γ which define R_{fp}. However, in the first vectorial expression of (2.5) only two out of three equations are independent, since $\mathbf{n}_1$ and $\mathbf{n}_2$ both have unitary norms. Thus, given R_{tf} and $\mathbf{P}_{tf}$, the system (2.5) makes it possible to find the relative poses of the patella and femur at each assigned flexion angle. It is worth noting that if the flexion angle is externally imposed, the PF motion depends from that of TF: this is an anatomical constraint which is satisfied in the model (system (2.5)).

Equations (2.5) and (2.2) are the closure equations of the knee joint in passive motion. They make it possible to find the relative poses of the patella, femur and tibia by assigning the flexion angle. As previously anticipated, points $\mathbf{C}_2$ and $\mathbf{D}_2$ have no influence on the closure equations of the mechanism in passive flexion. If the prismatic joint displacement s is required, it is sufficient to solve the position analysis problem and then to evaluate the distance between the points $\mathbf{C}_2$ and $\mathbf{D}_2$.

The 16 parameters which define the passive motion model of PF have to be identified in order to complete the first step of the sequential approach. The procedure of identification is described in section 3.2. The structures which guide the passive motion of PF are identified in the knee model as a result: they are not changed during the following steps, in order to observe the first rule of the sequential approach.

The final result of the first step of the proposed procedure is a set of 35+16 parameters which define a model of the passive motion of the whole knee and, at the same time, which constitute the first block of the sequential approach, i.e. the foundations on which the complete model of the knee has to be built. The preliminary model obtained from the first step can reproduce the passive motion only; the next steps of the procedure enrich this model by adding new anatomical structures, making it possible to reproduce the behaviour of the knee even under different loading conditions.

2.4 Second step: the stiffness model

The motions of the knee when static external loads are applied (muscular loads excluded) are considered in the second step of the proposed procedure. These problems are referred to both as quasi-static and as dynamic problems in the literature, in the sense that the motions of the joint are unknown, while the loads are given. They make it possible to identify several parameters connected to the stiffness of the passive structures of the knee — also including those not involved in the passive motion. At the same time, since the external loads do not include muscular forces, all parameters connected to the muscles must be ignored; moreover, since the loads are static, all parameters connected to time-varying quantities (as the inertia of the masses or the internal damping of the knee structures) must not be considered. These parameters can be identified in a further step of the sequential approach, as required by the first rule of the procedure.

All these considerations suggest to regard the motions produced by external loads as further basic tasks. They indeed meets the requirements of simplicity and relevance, as described in section 2.2.1: they emphasize the role played by a limited number of structures to stabilize the joint under some defined loading conditions; furthermore, they make it possible to ignore the presence of other structures and of other parameters which do not influence the considered motions. These tasks show the restraining capability of the passive knee structures, a fundamental characteristics for the restoration of the knee stability.

A further reason which leads to the choice of these motions as the basic tasks for the second step of the procedure is their anatomical and clinical significance. The analysis of the movement of the knee when subjected to external loads is indeed a common clinical practice to locate eventual damages or ruptures of the passive structures of the knee, since a high mobility of the joint is normally associated to these damages. Among the infinite combinations of external loads, it is thus advisable to choose loading conditions that reproduce these clinical tests. These tests indeed have been devised to stress all the passive structures of the knee, and they have been improved by the clinical practice to test and to analyse the stability of the joint. Thus, they are a well-founded reference to model the restraining structures of the knee.

Three out of the most common clinical tests are the *drawer*, the *torsion* and the *ab/adduction* tests. The first consists in applying an anteriorly or posteriorly directed load to the tibia and to analyse its anterior or posterior displacement at several flexion angles: the test has been devised in particular to stress the ACL and PCL, but several studies prove that the posterior structures of the knee also have an important role in restraining anterior-posterior displacements, thus affecting the test [12, 20]. The torsion test consists in applying a moment along the tibia longitudinal axis and to determine the internal/external rotation at several flexion angles: this loading condition is particularly useful to test the posterior structures and the collateral ligaments. The ab/adduction test consists in applying a moment to the tibia along its anterior axis in order to obtain an ab/adduction rotation which is analysed at several flexion angles: this test in particular stresses the collateral ligaments of the knee.

It is worth noting that all these tests — as the passive motion — can be carried out in vivo and, as a consequence, they make it possible to set the model parameters on a patient. This is a fundamental aspect when the knee model is used as a tool to assist surgical planning or prosthesis setting, as clarified in section 2.2.3. Moreover, this characteristic allows other important applications in the fields of clinical analysis and rehabilitation. The comparison between the results of the clinical tests obtained *in vivo* from a patient and those obtained from the model could provide significant insights for a correct and more precise diagnosis. In the common practice, these results are indeed qualitatively analysed, in general, and their interpretation is based on clinical experience; on the contrary, a clinical test model is a quantitative tool which could provide more objective and detailed results to identify damages or deficiencies in the passive structures of a patient's knee.

The drawer, torsion and ab/adduction tests are taken as a reference for the second step of the proposed procedure: the corresponding relative motions of the tibia, femur and patella are regarded as the basic tasks of this step. They make it possible to identify the stiffness characteristics of the passive structures of the joint. As a consequence, the final result of the second step of the sequential approach is the stiffness model of the knee.

2.4.1 The multi-fibre model

In order to define the stiffness model of the knee, a stiffness model of the passive structures is required. In the literature, several studies have modelled the stiffness characteristic of the knee and, in particular, some authors have defined models which can replicate the relative motion of the femur, tibia and patella during clinical tests. Some of them used 3D finite elements to model the visco-elastic properties of ligaments [2, 18, 23]; other authors used simple elastic line elements [4, 24, 25]. Since a detailed map of stress and strain of ligaments is not within the scopes of this dissertation, the second simpler approach is used instead. This simplified technique already proved to provide an accurate and sufficiently detailed description of the stiffness characteristic of the knee ligaments [5, 24].

Each ligament is modelled by means of a set of elastic fibres: each fibre in the model replaces a bundle of fibres of a ligament. This is why this method is known in the literature as *multi-fibre approach* (Figure 2.12). Despite the technique used for the stiffness model has already been proposed by other authors, the multi-fibre model presented in this dissertation contains some original contributions. The main difference lies on the definition of the fibres which constitute each ligament: the fibres are chosen on anatomical bases as in [24], but the application of the rules imposed by the sequential approach forces to use particular anatomical fibres also, i.e. the fibres which guide the passive motion. This aspect is clarified in the following. Furthermore, the sequential approach and the passive motion model which stems from the first step make it possible to originally extend the

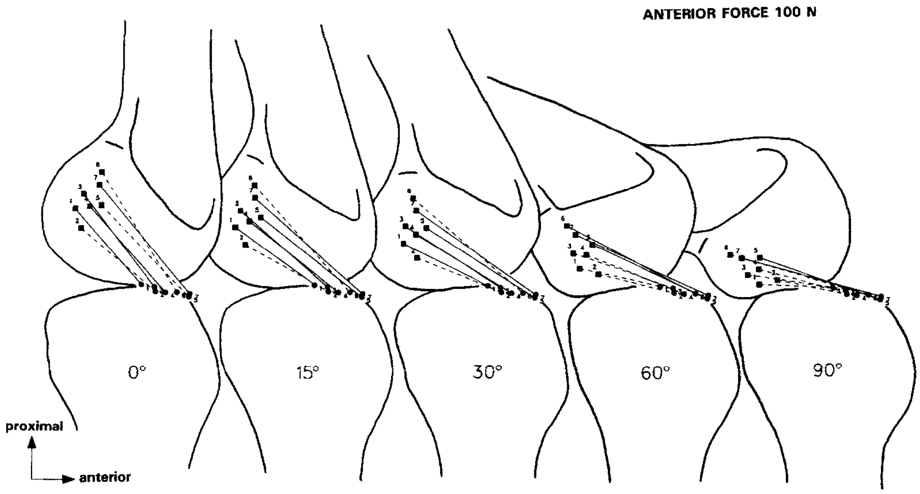

Figure 2.12: The multi-fibre model of a ligament [25].

multi-fibre approach for the modelling of the contacts between the femur and tibia condyles. Finally, the identification procedure based on optimization (section 3.2) shows some differences with respect to other papers in the literature, because of the rules of the proposed procedure (section 2.2).

Each fibre of the multi-fibre model considered in this dissertation is a simple line element which connects its attachments on the tibia and on the femur: fibre-fibre and fibre-bone interactions are not considered. The force exerted by each fibre j of a ligament is:

$$\begin{array}{ll} F_j = k_j\, \varepsilon_j^2 & \varepsilon_j > 0 \\ F_j = 0 & \varepsilon_j \leq 0 \end{array} \tag{2.6}$$

where k_j is a stiffness parameter and ε_j is the strain of the fibre:

$$\varepsilon_j = \frac{L_j - L_{0j}}{L_{0j}} \tag{2.7}$$

in which L_j and L_{0j} are respectively the length and the zero force length of the fibre, i.e. the limit length which divides tension (first equation of (2.6)) from laxity (second equation of (2.6)) conditions of a fibre. The F-ε relation (2.6) has been chosen among all those proposed in the literature for its simplicity: it is sufficient a single parameter to characterize a fibre; on the contrary, a linear-parabolic or an exponential relation — often used in the literature — requires two parameters [46]. It is worth noting that a fibre can actually intersect another fibre or a bone. The problem could be overcome by using fibre-fibre and fibre-bone contact models. Some simplified contact models have been proposed in the literature [3, 11] which can take into account some fibre-bone interactions; a more accurate model which can take into account also fibre-fibre contact has been recently proposed [7, 40].

These studies prove that fibre-fibre interactions have a limited influence on the model, while fibre-bone contacts can actually affect knee motion. Anyway, fibre contact models are not considered in this dissertation to simplify the knee model and reduce the computations of the identification procedure.

The described multi-fibre model is applied to the principal ligamentous structures of the knee, as reported in Table 2.1. The numbers of fibres of ACL, PCL and MCL are chosen in agreement with [24].

It is worth noting that only the stiffness characteristics of the passive structures of TF has been modelled. Since muscular loads are not considered in this step, the quadriceps and, as a consequence, the PT are not tight: the PF is in passive conditions and the model obtained from step one still holds (section 2.3.2). In particular, the relative motion of the patella and femur can be obtained from the system (2.5). Anyway, the motion is different from that obtained in the first step, since the relative poses of the femur and tibia (described by R_{tf} and $\mathbf{P}_{tf}$) are not the same as before: this is in agreement with experimental observations.

The stiffness model of ACL, PCL, MCL includes the IF also (section 2.3.1), which are obtained at the first step of the procedure. At the first step the IF are rigid links that guide the passive motion of TF. At the second step the IF are not rigid and can lengthen by following the F-ε law (2.6); even though they are not isometric any more, these fibres will be referred to as IF in the following, to differentiate them from the others. In order to obey the first rule of the sequential approach, the attachments of IF and their lengths L_{0j} remain those which have been identified at the first step. As a consequence, only parameters k_j have to be identified at the second step, as regards these fibres.

As regards the other fibres, both L_{0j} and k_j parameters must be identified; the attachments are not changed during the identification process to simplify computations. In order to obey the second rule of the sequential approach, L_{0j} lengths are inferiorly bounded: their minimum values are chosen so that these fibres are never tight in passive flexion. This requirement can be accomplished by choosing L_{0j}^{min} as the maximum distance reached by the fibre attachments in the passive model,

Ligaments	NoF	Anatomical information
Anterior cruciate (ACL)	5	Two fibres in the anterior bundle, two fibres in the posterior bundle, one IF.
Posterior cruciate (PCL)	5	Two fibres in the anterior bundle, two fibres in the posterior bundle, one IF.
Medial collateral (MCL)	6	Two fibres in the deeper bundle, three fibres in the superficial bundle, one IF.
Lateral collateral (LCL)	3	Uniformly distributed fibres.
Posterior structures	5	They include the arcuate ligament (one fibre), the popliteus tendon (two fibres) and the oblique popliteus ligament (two fibres).

Table 2.1: The ligaments and the number of fibres (NoF) used in the model.

during the considered flexion arc:

$$L_{0j}^{min} = \max\left\{ \left\| \mathbf{T}_j - R_{tf}^{\alpha_k}\mathbf{S}_j - \mathbf{P}_{tf}^{\alpha_k} \right\|,\ \alpha_k = \alpha_{min}, \ldots, \alpha_{max} \right\} \tag{2.8}$$

where $\mathbf{T}_j$ and $\mathbf{S}_j$ are the tibial and femoral attachments of a fibre, expressed in $\mathscr{S}_t$ and $\mathscr{S}_f$ respectively. This requirement guarantees that the passive motion is not influenced by the new fibres, as experimentally proved, and that results obtained at the first step are not modified.

The 5-5 mechanism used for the modelling of TF passive motion makes it possible to extend the multi-fibre approach to model the contact between the condyles. The contact model is indeed similar to that used for the ligamentous structures. The two rigid links that stand for the condylar contacts in the first step are now considered as deformable, in order to take into account the menisci strain and the possible bone separation. The F-ε model (2.6) can be used for medial condylar contact, while it must be slightly modified for lateral contact:

$$\begin{aligned} F_j &= -k_j\, \varepsilon_j^2 \quad && \varepsilon_j < 0 \\ F_j &= 0 && \varepsilon_j \geq 0 \end{aligned} \tag{2.9}$$

This is a consequence of the different concavity of the tibial and femoral condyles: the lateral condyles are both convex; the tibia medial condyle is concave, while the femur one is convex. This characteristic affects the relative position of the two attachments of each CF and, as a consequence, the direction of the constraints. A graphic explanation is given in Figure 2.13. The contact model could be refined by substituting the first of (2.9) with a more accurate F-ε law, but this aspect is outside the scope of this dissertation. The insertion points and L_{0j} lengths of the contact fibres remain those obtained at the first step, in order to satisfy the first rule of the sequential approach; the k_j parameters of CF are not identified in this study and are fixed at high values in order to simulate a quasi-rigid contact.

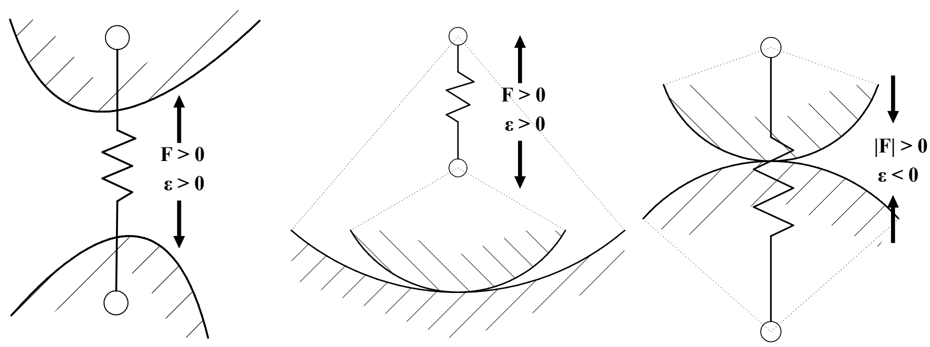

(a) Ligament (b) Concave-convex contact (c) Convex-convex contact

Figure 2.13: The relations between strains and forces of ligament (a), medial condyle (b) and lateral condyle (c) fibres of the proposed multi-fibre model.

This model shows to be a simplified approach, based on several approximations. In particular, it is assumed that the contact between each pair of condyles is a single point, that the spherical approximation of articular surfaces is still valid and that the CF are directed as the anatomical articular forces. At the same time, it proves to be sufficiently accurate and simple, making it possible to represent the contacts as all the other fibres, i.e. as non-linear springs which connect the femur and tibia.

A schematic representation of the stiffness model of the knee is reported in Figure 2.14. It can be regarded as the equivalent mechanism obtained from the first step of the proposed procedure, with the addition of a set of springs, representing the passive structures which do not influence the passive motion. When external loads vanish, the springs are all slack and cannot exert any forces: the relative motion of the tibia, femur and patella is guided by the equivalent mechanism. When external loads are imposed to the joint, some or all springs could become tight and exert forces; the equivalent mechanism is deformed by applied loads, as every mechanism does if elastic properties of its members are not ignored.

The relative poses of the femur and tibia can be obtained from the stiffness model by solving the equilibrium equations of the tibia. The tibia can be considered as a rigid body with six dofs, to which several loads are applied. In particular, the elastic forces of fibres can be obtained from:

$$\begin{aligned} \mathbf{F}_j &= F_j \frac{R_{tf}\mathbf{S}_j + \mathbf{P}_{tf} - \mathbf{T}_j}{L_j} \\ L_j &= \left\| R_{tf}\mathbf{S}_j + \mathbf{P}_{tf} - \mathbf{T}_j \right\| \end{aligned} \tag{2.10}$$

where F_j is the elastic modulus computed from (2.6) or (2.9), $\mathbf{T}_j$ and $\mathbf{S}_j$ are the tibial and femoral attachments of a fibre, expressed in $\mathscr{S}_t$ and $\mathscr{S}_f$ respectively. Other loads applied to the tibia are the tibia weight $\mathbf{F}_w$, the external force related to a clinical test $\mathbf{F}_{ext}$, the external torque related to a clinical test $\mathbf{M}_{ext}$ and a counterforce $\mathbf{F}_c$ which makes it possible to fix the flexion angle at a determined value. The forces are all expressed in $\mathscr{S}_t$. Thus, the equilibrium equations of the tibia are:

$$\begin{aligned} &\sum_{j=1}^{NoF} \mathbf{F}_j + \mathbf{F}_w + \mathbf{F}_{ext} + \mathbf{F}_c = \mathbf{0} \\ &\sum_{j=1}^{NoF} \mathbf{M}_{Oj} + \mathbf{M}_{Ow} + \mathbf{M}_{Oext} + \mathbf{M}_{Oc} + \mathbf{M}_{ext} = \mathbf{0} \end{aligned} \tag{2.11}$$

where NoF is the fibre number and $\mathbf{M}_{Oj}$, $\mathbf{M}_{Ow}$, $\mathbf{M}_{Oext}$, $\mathbf{M}_{Oc}$ are the moments of the corresponding forces, with respect to an arbitrary point $\mathbf{O}$, all expressed in $\mathscr{S}_t$.

If the flexion angle α is assigned, the system (2.11) is composed by six equations with six unknowns, i.e. the three components of $\mathbf{P}_{tf}$ the angles β, γ which define R_{tf} and the counterforce modulus F_c. These equations are numerically solved. As a result, the relative poses of the tibia and femur are obtained for each considered loading condition and each imposed flexion angle.

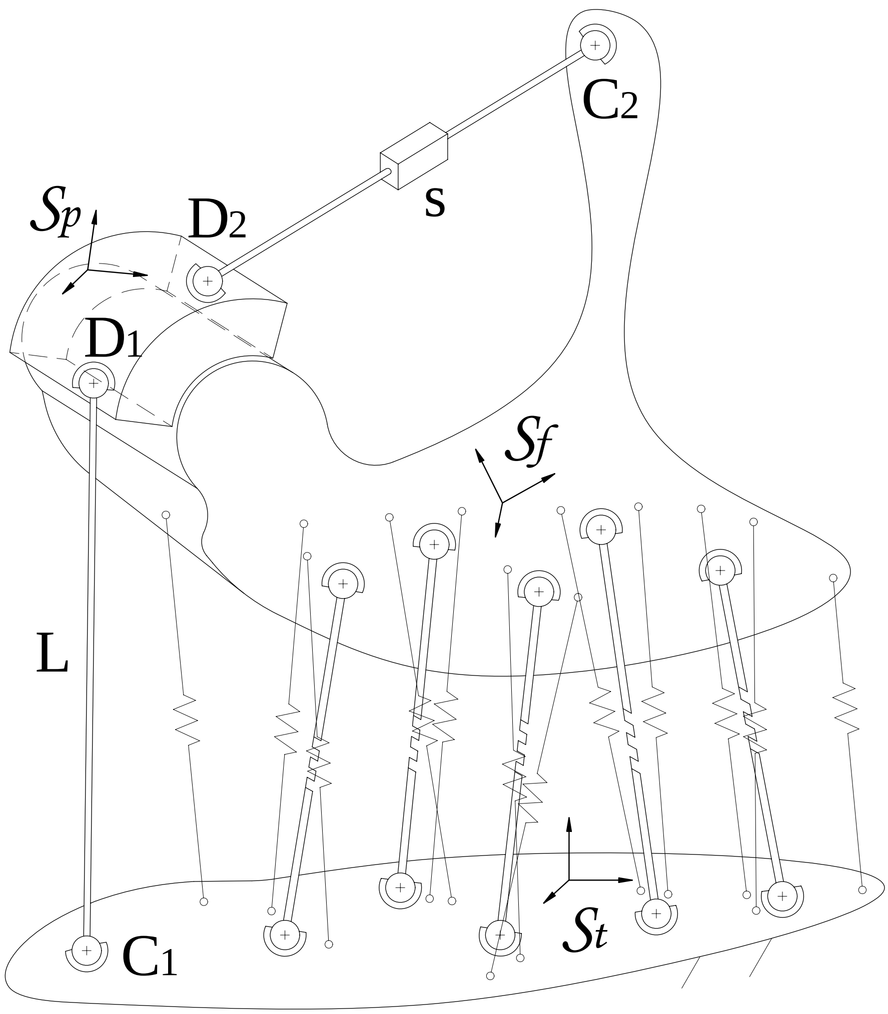

Figure 2.14: The stiffness model of the knee.

The identification of the 45 L_{0j} and k_j parameters of the fibres from experimental data leads to the definition of the stiffness model of the knee, which is also the result of the second step of the sequential approach. This model can replicate the passive motion with the same accuracy of the simpler model which resulted from the first step of the procedure. In addition, it can also replicate the motion of the articulation when external loads are applied.

2.4.2 An alternate approach for the contact modelling

The contact model presented in the previous section proves to be sufficiently accurate in all the tests performed for this dissertation. However there could be the need to use a more sophisticated description of the contacts between the anatomical surfaces.

The first reason lies in the approximations of the contact model, in particular those related to the direction of the contact forces. It is important indeed that these directions are close to the anatomical ones, in order to correctly replicate the loading conditions of the joint. The spherical approximation of the condyles and the following identification of the passive motion model could indeed alter the directions of contact forces excessively, in particular those exerted between the medial condyles. A second reason which could lead to consider a different approach for contact modelling is due to the strict connection between the simplified approach and the 5-5 model: if the passive motion of TF is described by means of a different mechanism (see for instance [37]), the simplified contact model cannot be used any more.

A more sophisticated description of the contacts can be obtained by means of a more accurate representation of the articular surfaces. As explained in section 2.3.1, equivalent mechanisms show numerical instabilities when the condyles are fitted by high-degree surfaces [28]. The problem can be overcome by means of a *reconstruction* of the articular surfaces during the second step of the procedure: articular contacts are modelled by means of low-degree surfaces for the modelling of the TF passive motion; they are then substituted by higher-order surfaces in the second step, in such a way that they are very close to the original anatomical shape.

This substitution requires some attention: it is fundamental that the new surfaces do not modify the passive motion which has been previously modelled, in order to obey the second rule of the sequential approach. In other words, the higher-order and the lower-order surfaces must be equivalent constraints for the passive motion mechanism. The simplest way to obtain higher-order surfaces which satisfy these constraints is to use *conjugate surfaces*: the anatomical femur condyles, for instance, can be approximated by higher-order surfaces, i.e. σ_1 and σ_2; the articular surfaces of the tibia, i.e. τ_1 and τ_2, are defined as their conjugate, with respect to the motion reproduced by the passive motion model. The two pairs of conjugate surfaces and the two pairs of lower-order surfaces constrain the passive model in a different but equivalent way.

The procedure can be clarified by means of an example, based on the experi-

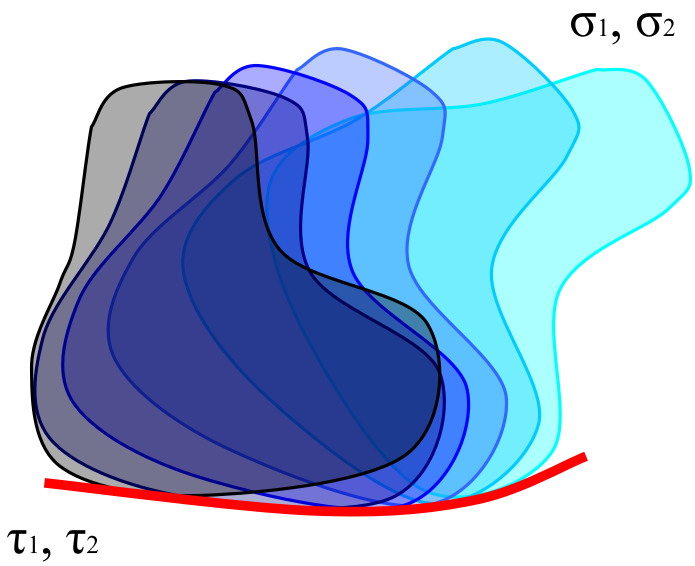

Figure 2.15: The envelope method for the definition of τ_1 and τ_2 (red), i.e. the conjugate surfaces of the given femoral condyles σ_1 and σ_2 (blue).

mental data described in section 3.1. The femoral condyles are approximated by two B-spline surfaces σ_1 and σ_2, with the help of the Rhinoceros 3D software. These surfaces are then imported into the Matlab computational environment and are jointed to the f rigid body of the 5-5 mechanism, which has been previously synthesized. The conjugate surfaces τ_1 and τ_2 on the tibia can be obtained by means of the envelope method, whose planar case is exemplified in Figure 2.15. The σ_1 and σ_2 condyles are moved by means of the 5-5 mechanism along a full passive flexion arc. The positions of these surfaces in $\mathscr{S}_t$ are collected and superimposed.

The 3D envelopes of all the positions of σ_1 and σ_2 are the corresponding conjugate surfaces on the tibia. The two envelopes τ_1 and τ_2 can be obtained by importing the superimposed positions of σ_1 and σ_2 into the Rhinoceros 3D software; these positions are then fitted by B-spline surfaces. Figures 2.16 and 2.18 show the superimposed positions of the medial and lateral condyles respectively. In particular, it can be noted that the envelopes (black edge) are very similar to the anatomical surfaces of the tibia (red lines). These observations are confirmed in Figures 2.17 and 2.19: the red surfaces are τ_1 and τ_2, while the red dots are the anatomical surfaces of the tibia. The envelopes are almost coincident with the real condyles: this is a confirmation of the accuracy of the 5-5 mechanism. On the contrary, the small differences make sure the new surfaces do not modify the motion of the passive model.

The τ_1, τ_2, σ_1 and σ_2 surfaces can be used to model the articular contacts in the stiffness model of the knee. The relative poses of the femur and tibia can be obtained by solving the equilibrium equations of the model; however, the sys-

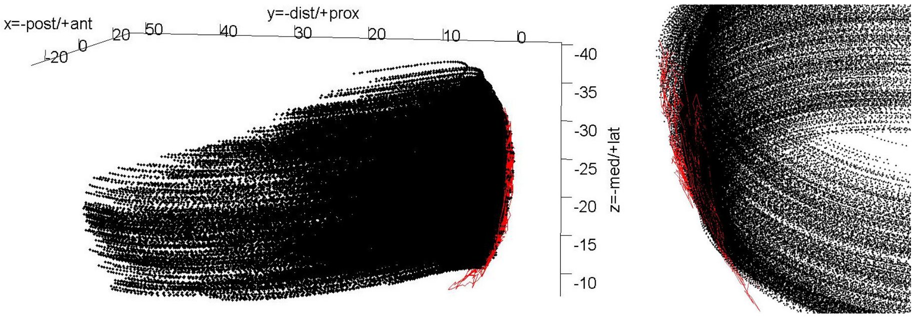

(a) Front view. (b) Lateral view.

Figure 2.16: Two views of the superimposed positions of the medial femoral condyle during passive flexion (black). Red lines represent the tibial anatomical condyle.

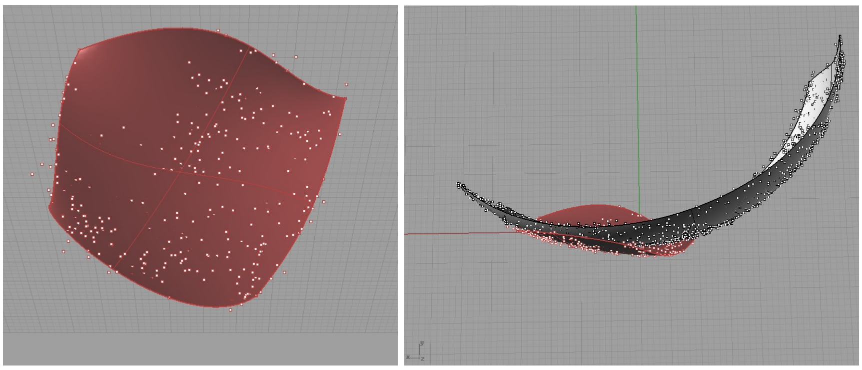

(a) The conjugate surface on the tibia. (b) The two conjugate surfaces.

Figure 2.17: The B-Spline approximation of the medial conjugate surfaces (red and black surfaces). Dots are the femur and tibia anatomical surfaces.

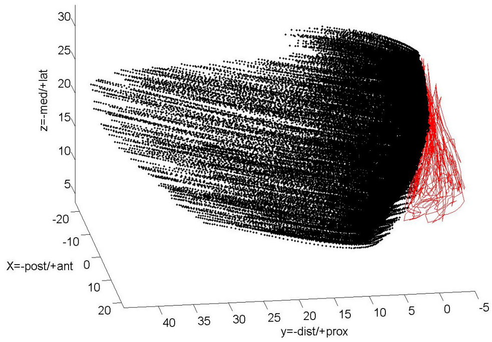

(a) Front view.

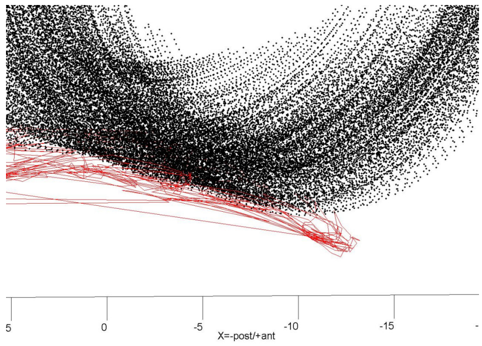

(b) Lateral view.

Figure 2.18: Two views of the superimposed positions of the lateral femoral condyle during passive flexion (black). Red lines represent the tibial anatomical condyle.

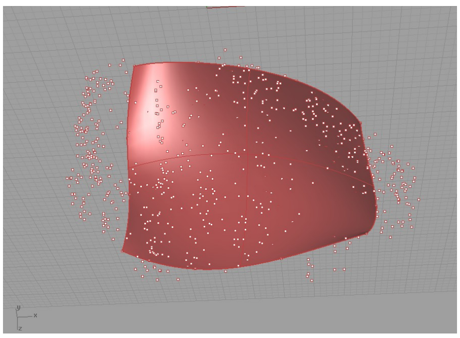

(a) The conjugate surface on the tibia.

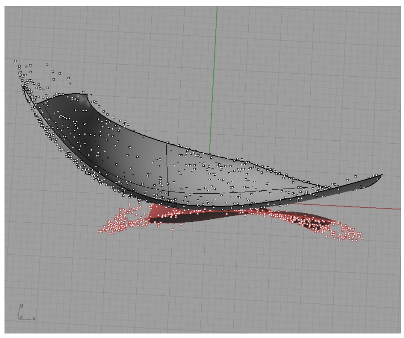

(b) The two conjugate surfaces.

Figure 2.19: The B-Spline approximation of the lateral conjugate surfaces (red and black surfaces). Dots are the femur and tibia anatomical surfaces.

tem (2.11) has to be modified to consider the alternate constraints imposed by the higher-order surfaces. If condyle deformations and bone separation are ignored, the equilibrium equations are:

$$
\begin{aligned}
&\sum_{j=1}^{NoF} \mathbf{F}_j + \mathbf{F}_w + \mathbf{F}_{ext} + \mathbf{F}_c + Q_1\mathbf{t}_1 + Q_2\mathbf{t}_2 = \mathbf{0} \\
&\sum_{j=1}^{NoF} \mathbf{M}_{Oj} + \mathbf{M}_{Ow} + \mathbf{M}_{Oext} + \mathbf{M}_{Oc} + \mathbf{M}_{ext} + \mathbf{M}_{OQ_1} + \mathbf{M}_{OQ_2} = \mathbf{0} \\
&\mathbf{T}_{\tau_1} = R_{tf}\mathbf{S}_{\sigma_1} + \mathbf{P}_{tf} \\
&\mathbf{T}_{\tau_2} = R_{tf}\mathbf{S}_{\sigma_2} + \mathbf{P}_{tf} \\
&\mathbf{t}_1 = R_{tf}\mathbf{s}_1 \\
&\mathbf{t}_2 = R_{tf}\mathbf{s}_2
\end{aligned}
\tag{2.12}
$$

where $Q_{1,2}$ are the contact force moduli; $\mathbf{M}_{OQ_{1,2}}$ are the corresponding momenta with respect to $\mathbf{O}$; $\mathbf{T}_{\tau_{1,2}}$ and $\mathbf{S}_{\sigma_{1,2}}$ are the contact points on $\tau_{1,2}$ and $\sigma_{1,2}$ respectively, expressed in $\mathscr{S}_t$ and $\mathscr{S}_f$; $\mathbf{t}_{1,2}$ and $\mathbf{s}_{1,2}$ are the unit vectors — expressed in $\mathscr{S}_t$ and $\mathscr{S}_f$ — which define the normal directions of $\tau_{1,2}$ and $\sigma_{1,2}$ in $\mathbf{T}_{\tau_{1,2}}$ and $\mathbf{S}_{\sigma_{1,2}}$. The other symbols have the same meaning described for equations (2.11).

The 3^{th} and 4^{th} vectorial equations of (2.12) constrain the contact points to be the same on the femur and tibia; the 5^{th} and 6^{th} vectorial equations constrain the normal directions to be the same at the contact points. Each surface can be defined by two coordinates: since contact points belong to these surfaces, both contact points and normal directions are a function of the corresponding two coordinates. Furthermore, since $\mathbf{t}_{1,2}$ and $\mathbf{s}_{1,2}$ have unitary norm, in the 5^{th} and 6^{th} vectorial equations only four out of the six components are independent. Thus, the system (2.12) is composed by 16 independent equations with 16 unknowns, i.e. the three components of $\mathbf{P}_{tf}$ the angles β, γ which define R_{tf}, the counterforce modulus F_c, the contact force moduli $Q_{1,2}$ and the 8 coordinates (2 for each surface) which define the contact points and the normal directions.

The solution of the equilibrium equations (2.12) makes it possible to find the relative position of the femur and tibia by means of the more sophisticated contact model. This model allows a better description of the contact forces, at the cost of a greater complexity of the problem. As previously noted, the simplified approach proves to be sufficiently accurate: this is why it is adopted in this dissertation. Anyway, the alternate approach described in this paragraph is a valid alternative for the modelling of more complex loading conditions.

2.5 The further steps

The model obtained in the second step of the procedure can accurately reproduce the passive motion and the stiffness of the knee. As a consequence, this model can be used to reproduce the relative motion of the tibia, femur and patella when the joint is subject to stationary external loads. The sequential approach could be extended to the modelling of more complex tasks, and, in particular, to dynamic problems comprising muscular and time-varying loads. In spite of these potentialities, the proposed procedure is not further extended in this dissertation. The main reason is connected to the lack of experimental data which are necessary to define and validate the more sophisticated models.

It is believed, however, that the two steps described in this chapter are sufficiently explanatory for the proposed procedure. They indeed lay the foundations of a dynamic model of the knee and show how to apply the fundamental rules and aspects of the sequential approach, which is the main subject of this dissertation.

In this sense, further developments of the model can be obtained by following the same indications provided in this chapter: other basic tasks have to be defined, in order to identify other parameters or other structures of the joint. For instance, time-varying external forces could be used to identify the internal damping of the passive structures; isometric contraptions of the muscles could be used to identify the parameters of one or few muscles at a time; and so on, until the definition of complex dynamic tasks which require the optimization of muscle activations. Each step enriches the knee model of new components; moreover, if the rules of the sequential approach are respected, previous results are not modified, preserving the restraining role of the joint structures, an aspect which is the foundation of the knee stability.

Chapter 3

The definition of model parameters

The passive motion model and the stiffness model of the knee proposed in the previous chapter are here identified from experimental data. The results are then presented to show the accuracy of the models and the effectiveness of the proposed procedure.

3.1 The acquisition of the anatomical data

In order to evaluate the accuracy of the knee model proposed in this dissertation, an experimental session was carried out at the Movement Analysis Laboratory of the Istituti Ortopedici Rizzoli (IOR), which provided also the experimental facilities and the indispensable surgical and technical assistance during the data acquisition. The photographic figures reported in the following pages were taken in that occasion.

The objective of the experimental session was collecting some geometrical data on a specimen which can be used to obtain a first approximation of the geometrical parameters that are necessary to define the knee model; furthermore, this session made it possible to record the experimental motion of the tibia, femur and patella during passive flexion. Since the experimental session was originally focused on the passive motion only, the relative motions of the tibia and femur during clinical tests were not recorded. On their place, the results reported in [12] are used as a reference, since the authors considered the same clinical tests as those of this dissertation and since the experimental results presented a relatively low standard deviation. Moreover, the anatomical conventions used in the reference paper are the same adopted in this dissertation: the tibia and femur reference system of [12] are very similar to those reported in section 2.1; the joint coordinate system used to represent relative rotations of $\mathscr{S}_f$ and $\mathscr{S}_t$ is the same [13]. This aspect helps to reduce the possible sources of error and to make the comparison between the results more sound.

Figure 3.1: The experimental setting for the acquisition of the anatomical and kinematic data.

A fresh-frozen right leg deriving from an amputation was analysed. The leg was declared as normal by the surgeon who assisted during data acquisition. The tibia was rigidly connected to a rigid frame to prevent any uncontrolled motion and to reduce the sources of error. On the contrary, the femur was not constrained and could be moved in a full flexion-extension arc. The contact between articular surfaces was ensured by a small load (40N) applied to the quadriceps by means of a dynamometer; the direction of the quadriceps force was declared as anatomical by the surgeon.

An opto-electronic system was used to digitalise the poses of three technical reference systems — rigidly attached to the tibia, femur and patella — with respect to a laboratory reference system. The experimental setting is shown in Figure 3.1. The three reference systems (whose tips are inserted into the bones) and the rigid frame can be easily recognized in the figure. The passive motion was obtained by approximately connecting the centre of mass of the femur to a cable (partially visible in Figure 3.1): the cable was wrapped around a pulley and it was then pulled with a low and almost constant velocity; the direction of the pull was nearly vertical. As a consequence, the loads on the joint were almost null.

A passive flexion-extension movement with range 5°–114° was recorded as a discrete succession of poses. The poses of each bone with respect to the laboratory reference system were given as sets of arrays of six parameters, three of them identifying the origin of the technical reference system and the others defining its orientation by means of Euler angles.

The knee was then anteriorly cut and the articular surfaces were exposed. The medial and lateral condyles of the femur and tibia, the trochlea and the front and back surfaces of the patella were digitalised by means of the same opto-electronic system (Figure 3.2). They were represented as clouds of points referring to their corresponding technical reference system. The same procedure was followed to digitalise the attachment areas of the ACL, PCL, MCL and LCL. These areas also were represented as clouds of points. Similarly, the position of the anatomical landmarks described in section 2.1.2 were recorded. This made it possible — during the following data analysis — to define the anatomical frames $\mathscr{S}_t$, $\mathscr{S}_f$, $\mathscr{S}_p$ and, at the same time, the matrices for the transformation of vector components from the technical to the anatomical systems. The points describing the articular surfaces and the ligament attachment areas were all projected into the respective anatomical frame. The anatomical surfaces and the ligament attachment areas are represented in Figures 2.3 and 3.3, together with $\mathscr{S}_t$, $\mathscr{S}_f$ and $\mathscr{S}_p$.

The attachment of the patellar ligament on the tibia was missing in the dataset, but it was reconstructed from the photographic material and from the data on the patella's articular surfaces. The posterior structures were not recorded — since they were not functional for the passive motion — and were thus obtained from the literature [43]. The stiffness parameters k_j were also obtained from the literature [5, 24].

As regards the passive motion, since the matrices for the transformation of vector components from the technical to the anatomical systems and those from the technical systems to the common laboratory one are known, the transformation matrices from $\mathscr{S}_f$ to $\mathscr{S}_t$ and those from $\mathscr{S}_p$ to $\mathscr{S}_f$ could be easily computed by simple transformation operators. Thus, the experimental matrices R_{tf}, R_{fp} and the experimental vectors $\mathbf{P}_{tf}$, $\mathbf{P}_{fp}$ could be obtained; they describe the relative poses of the tibia, femur and patella during the passive motion at each sampling point. Finally, by means of the joint coordinate system proposed in [13], the relative orientations between the femur and tibia and between the patella and femur were also

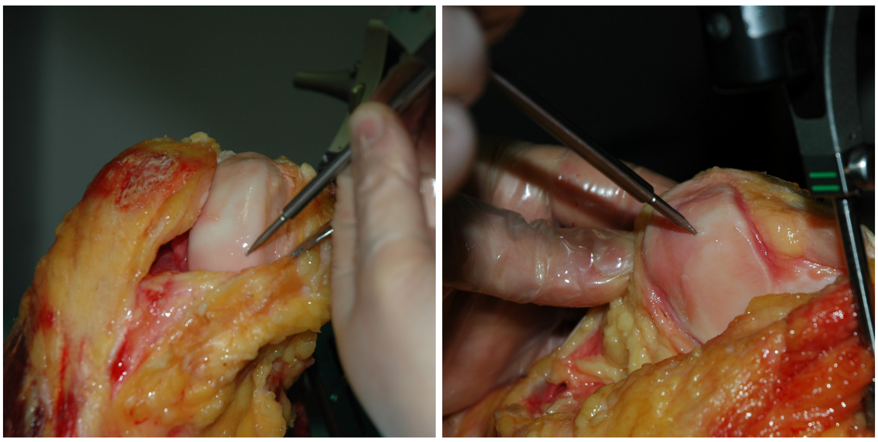

(a) The femur's medial condyle. (b) The patella's back surface.

Figure 3.2: The digitalisation of the anatomical surfaces by means of an optoelectronic system.

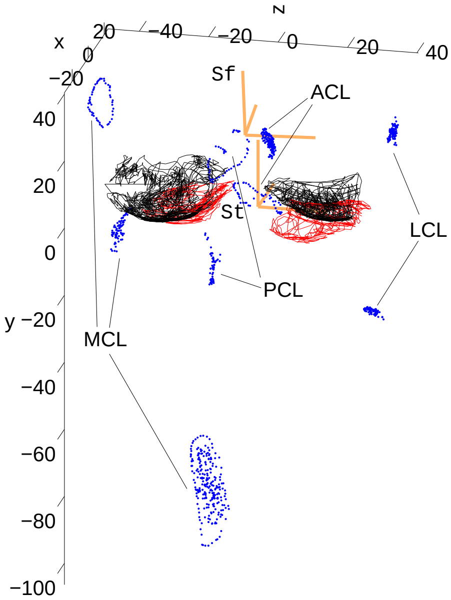

Figure 3.3: Condylar surfaces (red=tibia, black=femur), ligament attachment areas (blue) and anatomical frames (orange) of the considered specimen in complete extension.

converted as the result of three rotations: flexion/extension, abduction/adduction, intra/extra rotations (section 2.1.2). For the sake of conciseness, these data are shown together with the results, in the section 3.3.

As regards the clinical tests, no loaded motion was recorded during the experimental session, as previously noted, but the data reported in [12] are taken as a reference. It is worth noting that this paper does not report the full sets of six parameters which define the relative poses of the femur and tibia during clinical tests: only the clinically most relevant parameters are reported, i.e. the anterior/posterior relative translation for the drawer test, the internal/external relative rotation for the torsion test and the ab/adduction relative rotation for the ab/adduction test. Thus, only these data are used in the identification procedure, despite the stiffness model makes it possible to obtain the complete array of parameters which define each relative pose.

The reference paper reports a fourth test also, called by the authors "passive motion": it was obtained by moving the rigid frame of the authors' experimental setting (Figure 3.4), with no loads applied to the joint. However, the joint is not actually under unloaded conditions since the weight of the tibia is not balanced. This motion is used by the authors as a reference for their experimental results: in order to correctly compare these experimental results with those obtained from the stiffness model, it is necessary to simulate also this loading condition, i.e. the relative motion of the tibia and femur when only the tibia weight is applied. For the sake of conciseness, this loading condition is called *reference passive motion* in the following.

In particular, the experimental results provided in the reference paper are:

Drawer test An anterior force is applied to the tibia and the anterior position of the tibia with respect to the femur is obtained at several flexion angles; the anterior displacement from the corresponding pose of the reference passive motion is obtained at each flexion angle and is provided. The posterior displacements are obtained and provided similarly.

Torsion test An internal torque is applied to the tibia and the internal rotation of the tibia with respect to the femur is obtained at several flexion angles; the internal angular displacement from the full flexion pose of the reference passive motion is obtained at each flexion angle and is provided. The external angular displacements are obtained and provided similarly.

Ab/adduction test A force directed along the z-axis of $\mathscr{S}_t$ (from medial to lateral) is applied to the tibia and the abduction rotation of the tibia with respect to the femur is obtained at several flexion angles; the abduction angular displacement from the full flexion pose of the reference passive motion is obtained at each flexion angle and is provided. The adduction angular displacements are obtained and provided similarly.

The kinematical and anatomical parameters obtained from the experimental session and from the literature are fundamental data for the identification proce-

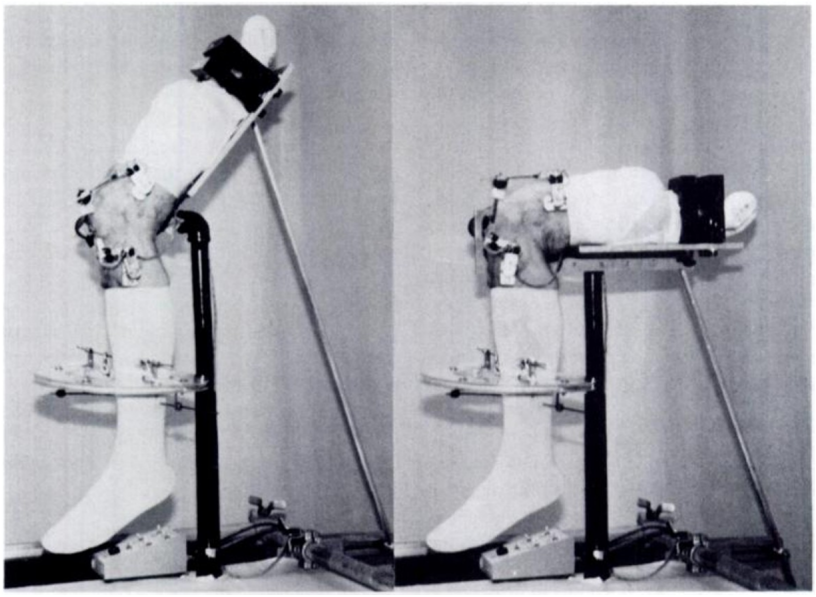

Figure 3.4: The experimental setting of the reference paper [12].

dure. The anatomical parameters make it possible to define a first approximation of the models; the kinematical information are used as a reference to adjust and to identify the model parameters.

3.2 The identification procedure

In order to define a model which can replicate the behaviour of the knee even under complex loading conditions, the physical relevance of the model should not be set aside. This means that the topology of the mechanism, its geometry and, as a consequence, its geometrical parameters should stem from experimental observations on the clinical and kinematical characteristics of the joint. This is an important point to relate the mathematical results of the model to the experimental ones, an aspect which becomes fundamental when the model is used for the study of the joint, for surgical purposes or for prosthetic design.

The lack of similarity between the model parameters and the anatomical or kinematical observations makes sure the restraining function of the knee structures is not correctly reproduced: the model could maybe replicate the behaviour of the knee under a given loading condition, but it is unlikely to give good results if a different task is prescribed. At the same time, the pursuit of total realism could be not only an excess, but could be also counterproductive. Approximations are often a need in a model, to reduce computational time and to allow a feasible identification procedure. Thus, some structures or some secondary characteristics could be ignored in the model: the other structures have to be slightly adapted to balance these necessary simplifications.

All these considerations lead to choose optimization as a method for the identification of the model parameters. In particular, bounded optimization procedures make it possible to find the parameter set which reduces to a minimum the errors between the experimental and the simulated motions, at the same time keeping the parameter values sufficiently close to the anatomical observations. Optimization techniques prove to be sufficiently flexible for this application and provide good results. On the contrary, other identification techniques based on precision points — as the Burmester theory — proved to be too rigid for this application and did not allow a good result to be obtained [39].

Both the passive motion and the stiffness models are identified by means of bounded optimization techniques. Starting from a first approximative solution (the first guess) deduced from the anatomical data, the optimum sets of 35+16 and 45 parameters are obtained which best-fit the experimental motions of the knee. Three distinct optimization problems are solved, i.e. the identification of the TF mechanism, that of the PF mechanism and the optimization of the stiffness model. The passive motion model could be identified in a single step: the choice of a two step optimization — permitted by the partial decoupling of the two sub-chains of the mechanism — simplifies the computations.

3.2.1 The first approximation of the models

A first approximation is required by the three optimization procedures as a starting point for the numerical research of the optimum solution. Since the first guesses are based on the anatomical remarks explained in sections 2.3 and 2.4, the optimum solutions have to be sufficiently close to the first guesses. Thus, the parameters of the first approximations are used also as a reference to define the domains of research, i.e. the bounds, for the optimization procedures.

The preliminary geometry of the 5-5 mechanism can be deduced from the experimental data. The relative positions of the ACL, PCL, MCL attachments from total extension to maximum flexion are analysed in passive conditions and for each ligament the pair of points (one on the femur and the other on the tibia) which show the minimum change in distance (isometric fibre) is chosen. The three points on the tibia ($\mathbf{A}_1$, $\mathbf{A}_2$ and $\mathbf{A}_3$) and those corresponding on the femur ($\mathbf{B}_1$, $\mathbf{B}_2$ and $\mathbf{B}_3$) are the centres of the spherical pairs on three of the five legs of the equivalent mechanism. The four condyles are then replaced by four best-fitting spheres whose centres ($\mathbf{A}_4$, $\mathbf{A}_5$ on the tibia and $\mathbf{B}_4$, $\mathbf{B}_5$ on the femur) are also the centres of the two remaining legs. The best-fitting spheres are determined by means of a standard least-square algorithm. The length L_{0i} of each leg is the distance between the spherical pairs on each link at the initial position (full extension). The preliminary geometry of the 5-5 mechanism obtained from the experimental data is shown in Figure 3.5 (black

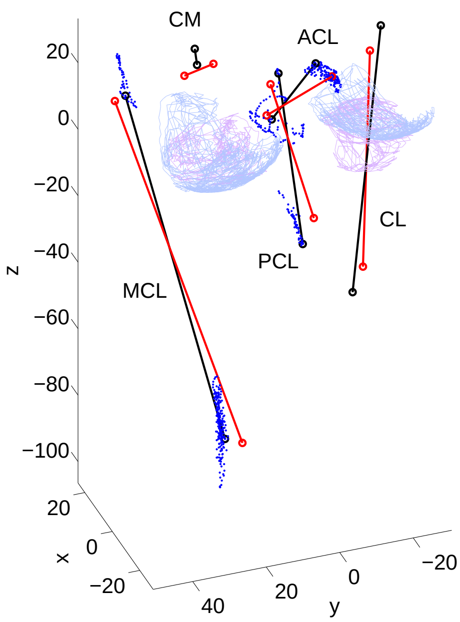

Figure 3.5: Rigid links of the 5-5 mechanism. The black lines are the links derived directly from the experimental data; the red ones represent the same links after the optimization.

Geom. parameters	$\mathbf{A}_1$ - ACL (mm)			$\mathbf{A}_2$ - PCL (mm)			$\mathbf{A}_3$ - MCL (mm)			$\mathbf{A}_4$ - CL (mm)			$\mathbf{A}_5$ - CM (mm)		
	A_{x1}	A_{y1}	A_{z1}	A_{x12}	A_{y2}	A_{z2}	A_{x3}	A_{y3}	A_{z3}	A_{x4}	A_{y4}	A_{z4}	A_{x5}	A_{y5}	A_{z5}
Preliminary estimate	17.80	-3.82	-0.72	-23.92	-15.33	-7.88	17.82	-97.18	-13.45	3.81	-51.26	16.05	0.89	33.29	-27.99
Optimized values	*13.30*	0.68	-3.80	-19.92	*-10.83*	*-3.38*	14.65	-97.29	-9.88	*8.31*	-47.21	*20.55*	-3.61	*28.79*	*-32.49*

Geom. parameters	$\mathbf{B}_1$ - ACL (mm)			$\mathbf{B}_2$ - PCL (mm)			$\mathbf{B}_3$ - MCL (mm)			$\mathbf{B}_4$ - CL (mm)			$\mathbf{B}_5$ - CM (mm)		
	B_{x1}	B_{y1}	B_{z1}	B_{x12}	B_{y2}	B_{z2}	B_{x3}	B_{y3}	B_{z3}	B_{x4}	B_{y4}	B_{z4}	B_{x5}	B_{y5}	B_{z5}
Preliminary estimate	-6.44	4.84	6.53	1.83	-2.27	0.23	1.48	4.66	-43.63	-1.09	6.62	27.62	2.63	7.21	-22.78
Optimized values	-8.06	0.51	10.50	-2.66	-1.16	-4.23	1.15	4.21	-46.77	-4.23	*2.12*	*23.12*	2.28	6.37	*-18.28*

Geom. parameters	L_1 - ACL (mm)	L_2 - PCL (mm)	L_3 - MCL (mm)	L_4 - CL (mm)	L_5 - CM (mm)
	—	—	—	—	—
Preliminary estimate	36.56	44.29	128.09	79.47	5.59
Optimized values	29.28	35.47	128.88	70.35	11.55

Table 3.1: Geometrical parameters of the TF model: $\mathbf{A}_i$ $(i = 1, \ldots, 5)$ refer to $\mathscr{S}_t$; $\mathbf{B}_i$ $(i = 1, \ldots, 5)$ refer to $\mathscr{S}_f$; CL and CM are the lateral and medial condyles. For each parameter, both the preliminary estimate and the final optimized value are reported. Numbers in italics are the parameters which lie on the bounds of the domain.

links), and the corresponding parameters are reported in Table 3.1. The values assumed by the same parameters after optimization are reported also (this procedure is described in the next section).

An estimate of the parameters of the PF equivalent mechanism can be deduced from the experimental data by considering the physical foundations of the model, described in section 2.3.2. The femoral articular surfaces of PF are approximated by a best-fitting cylinder in $\mathscr{S}_f$: the axis of the cylinder makes it possible to obtain $\mathbf{n}_1$ and $\mathbf{Q}_1$. The projections of these vectors in $\mathscr{S}_p$ (an intermediate relative pose between the patella and femur is chosen) allow $\mathbf{n}_2$ and $\mathbf{Q}_2$ to be defined; the distance between $\mathbf{Q}_1$ and $\mathbf{Q}_2$ sets the λ parameter. Finally, the attachment areas of the patellar ligament are analysed: the pair of points — the first on the tibial attachment, the other on the patellar one — which exhibits the lowest change in distance during the experimental movement (isometric fibre) defines the points $\mathbf{C}_1$ and $\mathbf{D}_1$; their mean distance sets the L length. The preliminary estimate of the geometrical parameters obtained on the considered specimen is reported in Figure 3.6 (black lines) and Table 3.2. The values assumed by the same parameters after optimization are reported also.

The elastic fibres required by the stiffness model are chosen as described in Table 2.1, starting from the collected attachment areas. In particular, great attention is devoted to the choice of anatomical and anatomically oriented fibres [9, 14, 24, 43]; the IF and CF are the result of the passive motion model. The complete elastic model is reported in Figure 3.7, where the IF and CF are emphasized. A first estimate of k_j parameters are taken from the literature [5, 24, 31]; the first estimate of the length L_{0j} of each fibre (excluding IF and CF, whose lengths are not optimized) are deduced from the passive motion model, as in equation (2.8). The loading conditions are chosen as close as possible to those reported in the reference paper [12], in order to have a significant comparison between experimental and simulated results. For the sake of conciseness, the numerical values of the parameters are not reported here.

3.2.2 The optimization procedure

The preliminary estimate of the geometrical and stiffness parameters is only a rough approximation of the final model: in order to best-fit the experimental results, these parameters have to be optimized. The model which stems from each step of the sequential approach must be optimized separately from the others, as a requirement of the proposed procedure. Thus, two optimization problems have to be solved at least, in order to identify the models defined at the first two steps of the sequential approach. However, as previously noted, despite the optimization procedure of the passive motion model could be extended to the whole mechanism, a two-step sequential optimization of the two sub-chains is preferred here just to simplify the procedure, since the final results would be very similar to the presented ones.

The optimization technique applied to the TF and PF mechanisms and that ap-

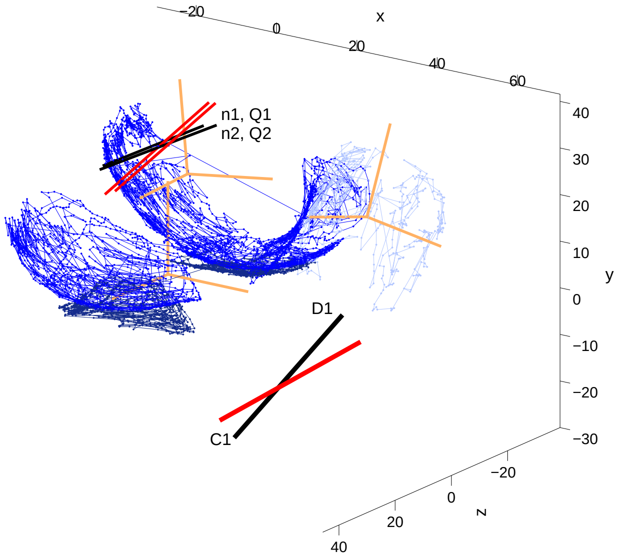

Figure 3.6: The preliminary estimate of the geometrical parameters (black lines) compared to the optimized ones (red lines). The blue clouds of points are the articular surfaces of the patella, femur and tibia.

Geom. parameters	$\mathbf{n}_1$ (rad)		$\mathbf{Q}_1$ (mm)		$\mathbf{C}_1$ (mm)			L (mm)
	δ_1	η_1	Q_{x1}	Q_{y1}	C_{x1}	C_{y1}	C_{z1}	L
Preliminary estimate	0.09	0.09	4.77	10.47	20.00	-30.00	5.00	48.67
Optimized values	-0.13	0.06	6.46	*15.47*	19.88	*-25.00*	*10.00*	40.02
Geom. parameters	$\mathbf{n}_2$ (rad)		$\mathbf{Q}_2$ (mm)		$\mathbf{D}_1$ (mm)			λ (mm)
	δ_2	η_2	Q_{x2}	Q_{y2}	D_{x1}	D_{y1}	D_{z1}	λ
Preliminary estimate	-0.13	0.19	-42.48	6.18	0.00	-21.00	0.00	-2.68
Optimized values	-0.30	0.29	-44.1	10.40	2.41	*-26.00*	*-5.00*	-1.76

Table 3.2: Geometrical parameters of the PF model: $\mathbf{n}_1$, $\mathbf{Q}_1$ refer to $\mathscr{S}_f$, $\mathbf{C}_1$ to $\mathscr{S}_t$ and $\mathbf{n}_2$, $\mathbf{Q}_2$, $\mathbf{D}_1$ to $\mathscr{S}_p$. For each parameter, both the preliminary estimate and the final optimized value are reported. Numbers in italics are the parameters which lie on the bounds of the domain.

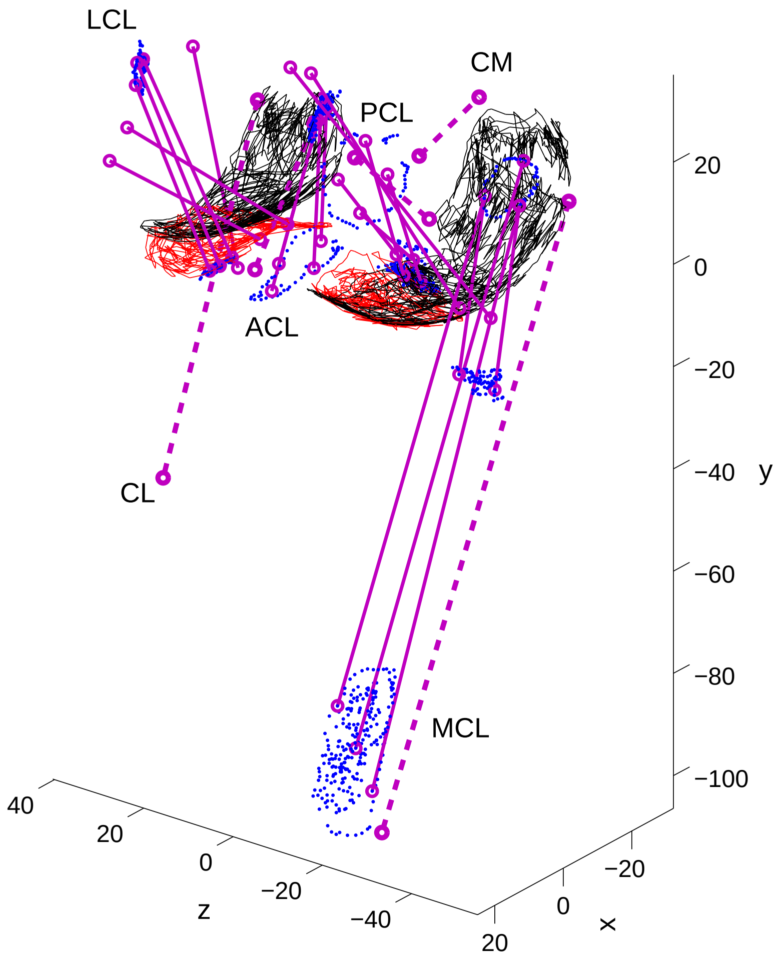

Figure 3.7: The stiffness model of the knee. Dotted lines are the isometric (IF) and contact (CF) fibres (corresponding to members $\mathbf{A}_i\mathbf{B}_i$ $(i = 1, \ldots, 5)$ of the 5-5 mechanism).

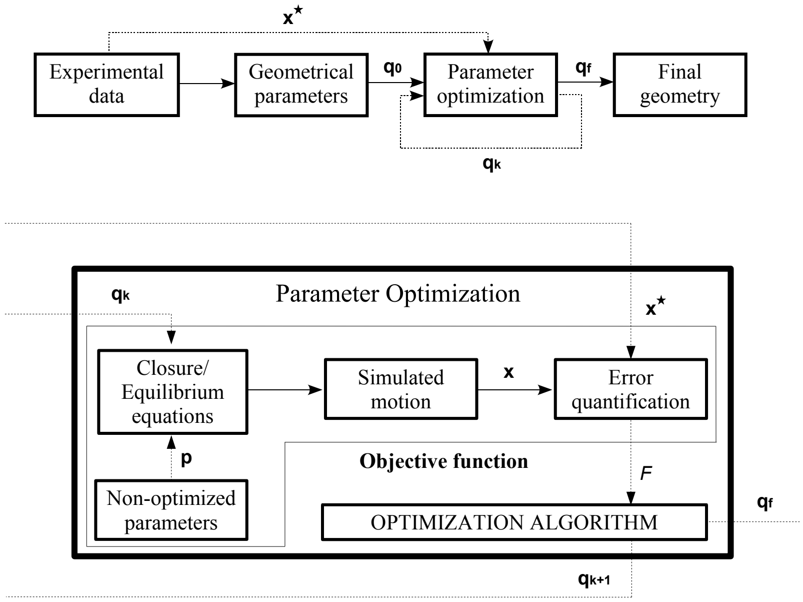

Figure 3.8: The optimization procedure for the identification of the passive motion and stiffness models.

plied to the stiffness model are substantially similar (Figure 3.8). The first guess $\mathbf{q}_0$ is passed to an objective function. The model is defined within the function, by means of $\mathbf{q}_0$ and other parameters (vector $\mathbf{p}$ in the figure) which are not optimized. The passive or loaded motions of the joint are obtained by solving the closure or equilibrium equations at the given flexion angles; the simulated motions $\mathbf{x}$ are then compared to the experimental ones $\mathbf{x}^\star$ and the differences are quantified by an index F. The value of this index leads the optimization algorithm to define a second guess $\mathbf{q}_1$ (compatible with the bounds) which is passed again to the objective function. The iteration is repeated until the minimum value of F is reached. The final parameter set $\mathbf{q}_f$ is the solution of the optimization problem.

As regards the 5-5 mechanism, twelve equally-spaced flexion angles are chosen in the experimental movement from complete extension to maximum flexion. At each optimization iteration, the closure equations (2.2) are solved at the twelve chosen angles. The relative poses of the femur and tibia computed from the model are iteratively compared with the experimental ones: the sum of the weighted squares of errors between the poses constitutes the error index F which has to be minimized. In particular, if x_{ji} is the computed value of the j^{th} unknown ($j = 1, \ldots, 5$) of the system (2.2), obtained at the i^{th} flexion angle ($i = 1, \ldots, 12$), the contribution of x_{ji} to the value of F is:

$$\varepsilon_{ji} = \frac{\left(x_{ji} - x^\star_{ji}\right)^2}{x^2_{jd}} \tag{3.1}$$

where $x^{\star}_{ji}$ is the corresponding experimental value of the unknown. The weights x_{jd} are necessary, since the unknowns have different physical dimensions (some are angles, others are lengths). The weights only depend on the unknown and are chosen as:

$$x_{jd} = \max\left\{x_{ji},\ i = 1,\ldots,12\right\} - \min\left\{x_{ji},\ i = 1,\ldots,12\right\} \tag{3.2}$$

Thus, the error ε_{ji} is a sort of per cent error, with respect to the maximum range x_{jd} of the j^{th} pose parameter.

The mechanism closure is not guaranteed for every parameter set: if the model closures are not satisfied at all the given flexion angles, an arbitrary high value is assigned to the index F. Thus, the complete algorithm for the computation of F is:

$$\begin{aligned} F &= \sum_{j=1}^{5}\sum_{i=1}^{12}\varepsilon_{ji} && \text{if closure succeeds} \\ F &= X && \text{otherwise} \end{aligned} \tag{3.3}$$

where X is an arbitrary high value. As previously noted, in order to give the proposed model a physical consistency, the optimization research domain is bounded, having the starting guess as the central value: every parameter q_n $(n = 1,\ldots,35)$ has to fall within the interval $[q_{0n} - \delta_n,\ q_{0n} + \delta_n]$.

The objective function is highly non-linear and, because of the bifurcation of (3.3), it presents many discontinuities. Quasi-Newton methods are powerful optimization algorithms which can efficiently find the minimum value of non-linear functions; unfortunately — like all deterministic algorithms which make use of derivatives of the objective function — they show numerical instabilities when solving discontinuous problems. Thus, a first approximation of the optimum solution is found by means of a heuristic algorithm, i.e. a genetic algorithm, which does not make use of derivatives. The bounded genetic algorithm makes it possible to find a feasible solution within the bounds, i.e. a geometry of the 5-5 parallel mechanism whose closures are satisfied at all the given flexion angles. The preliminary solution is then iteratively refined by means of a quasi-Newton algorithm: the search for the optimum solution is carried out by "guiding" the minimum on even bigger domains inside the bounds and by keeping the algorithm on continuous zones of the objective function.

The results of the identification of the 5-5 mechanism are reported in Figure 3.5 (red links) and in Table 3.1. The optimized model is very close to the first estimate: this aspect gives consistency to the kinematical and anatomical assumptions which lead to the definition of the TF equivalent mechanism.

As regards the PF equivalent mechanism, twelve equally-spaced experimental flexion angles are chosen in order to span the complete passive movement of the knee. The corresponding experimental relative poses between the patella and femur are selected. Otherwise, the relative poses of the femur and tibia are obtained from the previously optimized TF model. These simulated poses are used to solve the closure equations (2.5) of the PF sub-chain at each given flexion angle. The solutions are then compared to the experimental poses of the patella and femur. The optimization procedure and the computation of the F error index are very similar to those used to identify the TF model. It is worth noting, however, that the simplicity of the PF equivalent mechanism makes sure the model closures are satisfied at each considered flexion angle, within the bounds. As a consequence, the objective function is continuous within the bounds and the optimum solution can be searched by means of quasi-Newton algorithms. The F error index can be obtained by:

$$\begin{aligned} \varepsilon_{ji} &= \frac{\left(x_{ji} - x^{\star}_{ji}\right)^2}{x^2_{jd}} \\ F &= \sum_{j=1}^{6} \sum_{i=1}^{12} \varepsilon_{ji} \end{aligned} \tag{3.4}$$

where the symbols have the same meaning as in (3.3). Apart from the missing bifurcation, the only difference from the TF model is the number of pose parameters which are fitted, i.e. 6 instead of 5. Contrary to the TF flexion angles, the patellar α rotation indeed is not imposed in the PF mechanism, whose motion is completely defined by the motion of the TF equivalent mechanism. In order to preserve the physical foundations of the proposed model, the parameter domain of research is bounded, the preliminary estimate of parameters being its centre: every parameter q_n ($n = 1, \ldots, 16$) has to fall within the interval $[q_{0n} - \delta_n,\ q_{0n} + \delta_n]$. The results of the optimization procedure are reported in Figure 3.6 and in Table 3.2.

Finally, as regards the stiffness model, the same flexion angles considered in the reference study are chosen, i.e. 0, 15, 30, 45, 60, 75, 90 degrees. At each optimization iteration, the equilibrium equations (2.11) are solved for the seven loading conditions. The loading conditions are those corresponding to anterior, posterior, internal, external, abduction, adduction loads, with the addition of the reference passive motion. The equilibrium equations are solved at 0 degrees of flexion; they are then solved at seven intermediate flexion angles before reaching the second given flexion angle, i.e. 15 degrees; the same procedure is repeated for all the given flexion angles. An intermediate result is used as a first guess to numerically solve the equilibrium equations at the following flexion angle: this procedure makes it possible to improve the stability of the solution. Anyway, only the results obtained at the seven given flexion angles are used for the computation of the error index F: the relative poses of the femur and tibia computed from the model are iteratively compared with the experimental ones, and the error index F is obtained as in (3.4), using $j = 1, \ldots, 7$ and $i = 1, \ldots, 7$ instead.

As previously noted, only k_j and L_{0j} parameters are optimized. The bounds are different from the previous optimization problems. Every stiffness parameter k_j has to fall within the interval $[0,\ k_{0j} + \delta_j]$, where k_{0j} is the value obtained from the literature. These data are affected by large dispersions, thus a higher variability is admitted for stiffness parameters. Every length L_{0j} has to fall within the interval

$\left[L_{0j}^{min}, L_{0j}^{min} + \xi_j\right]$, where L_{0j}^{min} can be obtained from (2.8), in order to respect the second rule of the sequential approach.

The high number of fibres reduces the stability of the equilibrium problem. In spite of the intermediate steps, the optimization algorithm could jump among the alternative solutions of the equilibrium equations during the search for the minimum value of F. As a result, the objective function is not smooth and quasi-Newton methods show numerical instabilities. A genetic algorithm is used instead and the solution is refined by means of another heuristic method, i.e. a direct search algorithm. These algorithms slow down computations, but they make it possible to obtain an optimum. The instabilities could be reduced by using a lower number of elastic fibres to describe each ligament: as previously noted, the number of fibres is chosen in agreement with [24]; however, an investigation could be carried out to define the minimum fibre number which makes it possible to correctly replicate the stiffness properties of the knee, at the same time reducing the instabilities of the equilibrium problem.

The optimum parameter sets represent the final result of the identification procedure. The accuracy and the motions of the models obtained from the first two steps of the sequential approach are presented in the next section.

3.3 Results

The position and rotation components of $\mathscr{S}_f$ in $\mathscr{S}_t$ during passive motion are presented in Figures 3.9 and 3.10: the dotted lines are the experimental data, while the solid ones are the results of the 5-5 mechanism. The position and rotation components of $\mathscr{S}_p$ in $\mathscr{S}_f$ during passive motion are similarly presented in Figures 3.11 and 3.12. The rotation components are the angles α, β and γ as defined in section 2.1.2; position components are expressed as x, y, z components of $\mathbf{P}_{tf}$ and $\mathbf{P}_{fp}$ vectors, respectively.

These results show that the proposed equivalent mechanism of the knee joint can accurately reproduce the relative motion of the tibia, femur and patella in passive flexion. The 5-5 parallel mechanism proves to be an optimal tool to replicate the passive flexion of TF with great accuracy. The PF model makes it possible to reproduce the experimental results with a good accuracy, while its simplicity makes it possible to solve the closure equations and the optimization procedure with a reduced computational time. In particular, the high mobility of the proposed model and its stability reduce the problems connected to the non-existence of closure equation solutions, and their consequences on the continuity of the objective function.

The results of the stiffness model are reported in Figures 3.13, 3.14 and 3.15. The motion of the tibia with respect to the femur is considered now, in order to use the same conventions of the reference paper. For the same reason, the position components are anterior/posterior anatomical displacements as defined in [13].

Higher and lower curves are the experimental (dotted lines) and simulated

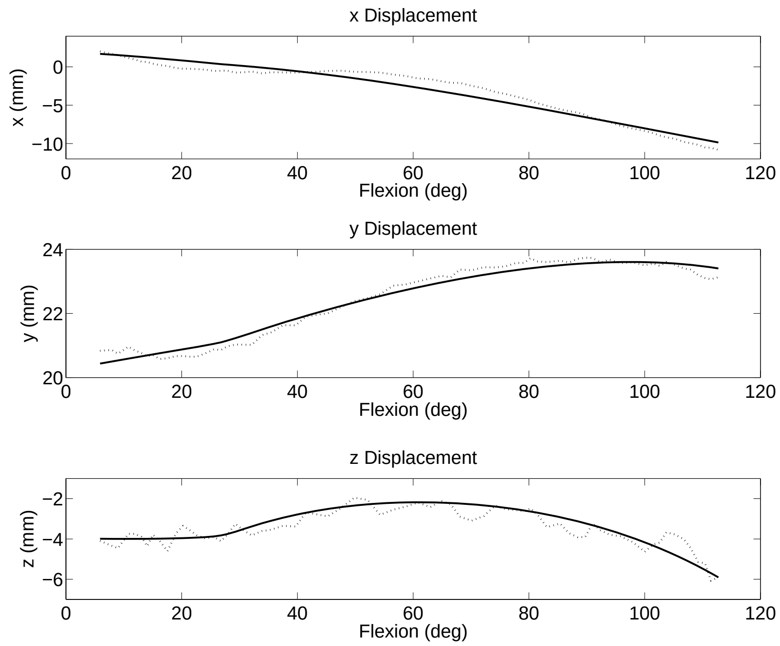

Figure 3.9: Position of $\mathscr{S}_f$ with respect to $\mathscr{S}_t$. Results of the 5-5 mechanism (solid) compared with the experimental data (dot).

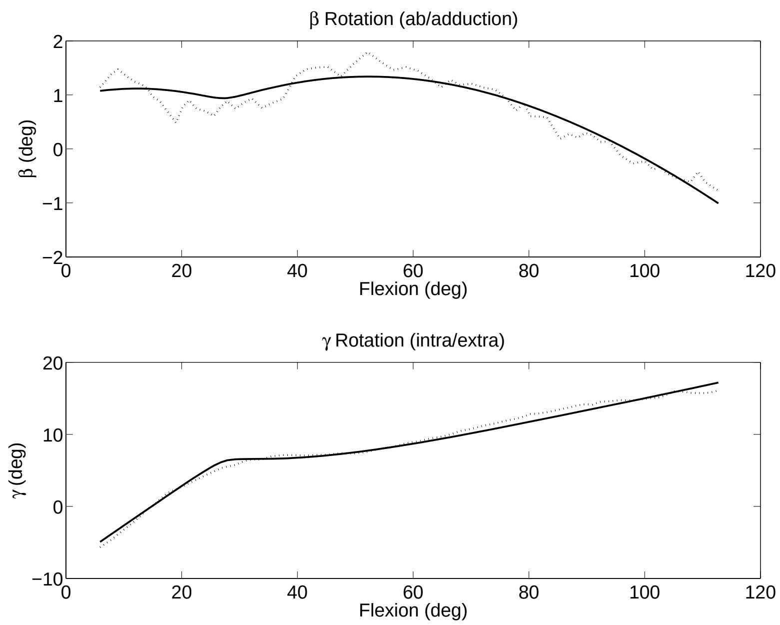

Figure 3.10: Orientation of $\mathscr{S}_f$ with respect to $\mathscr{S}_t$. Results of the 5-5 mechanism (solid) compared with the experimental data (dot).

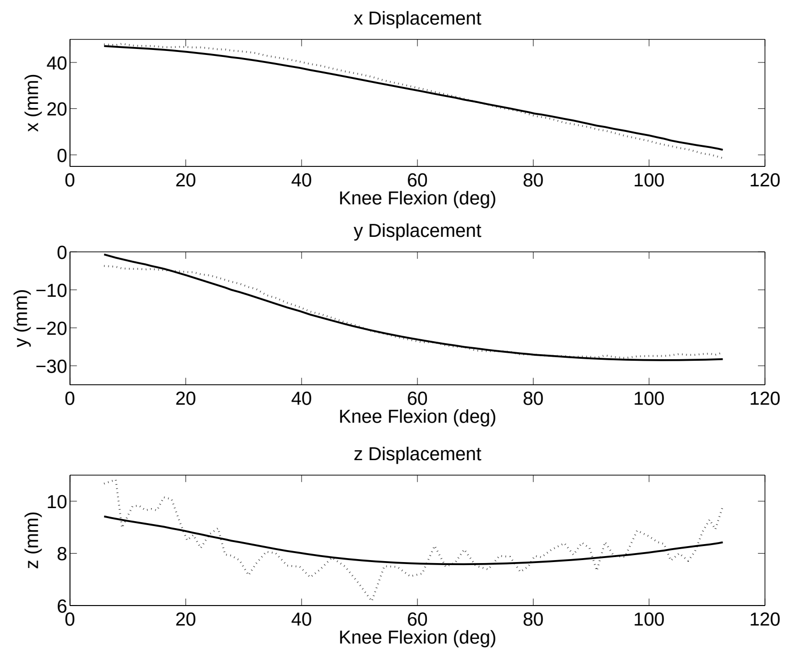

Figure 3.11: Position of $\mathscr{S}_p$ with respect to $\mathscr{S}_f$. Results of the PF equivalent mechanism (solid) compared with the experimental data (dot).

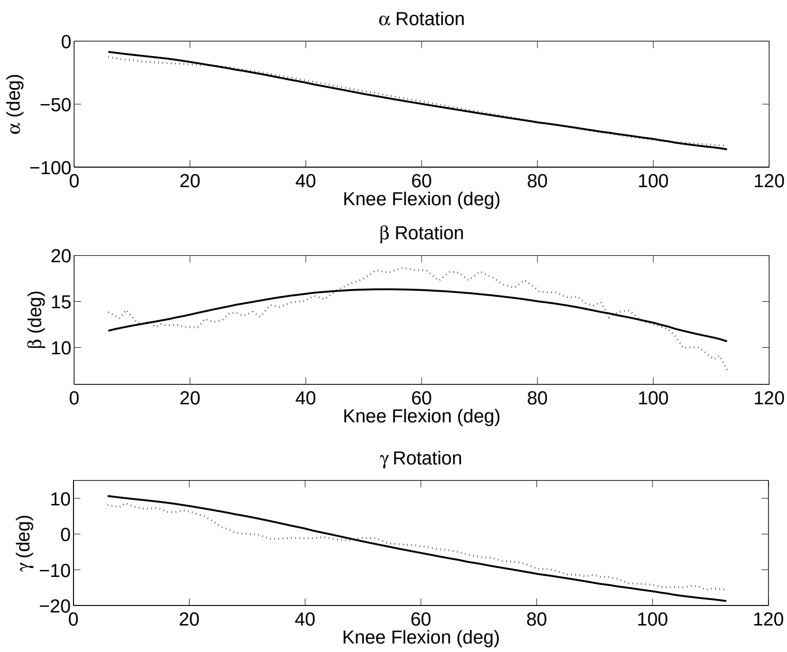

Figure 3.12: Orientation of $\mathscr{S}_p$ with respect to $\mathscr{S}_f$. Results of the PF equivalent mechanism (solid) compared with the experimental data (dot).

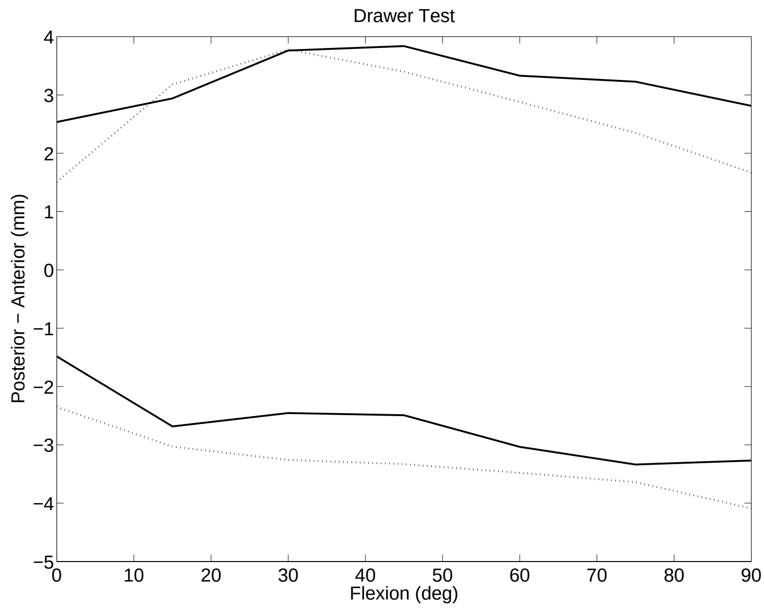

Figure 3.13: Posterior/anterior displacements of $\mathscr{S}_t$ with respect to $\mathscr{S}_f$. Results of the stiffness model (solid) compared with the experimental data of the reference paper (dot).

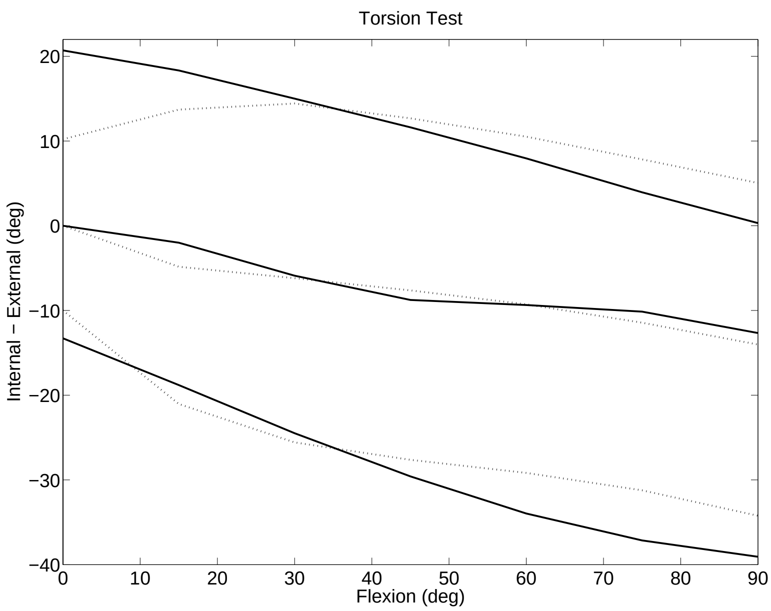

Figure 3.14: Internal/external angular displacements of $\mathscr{S}_t$ with respect to $\mathscr{S}_f$. Results of the stiffness model (solid) compared with the experimental data of the reference paper (dot).

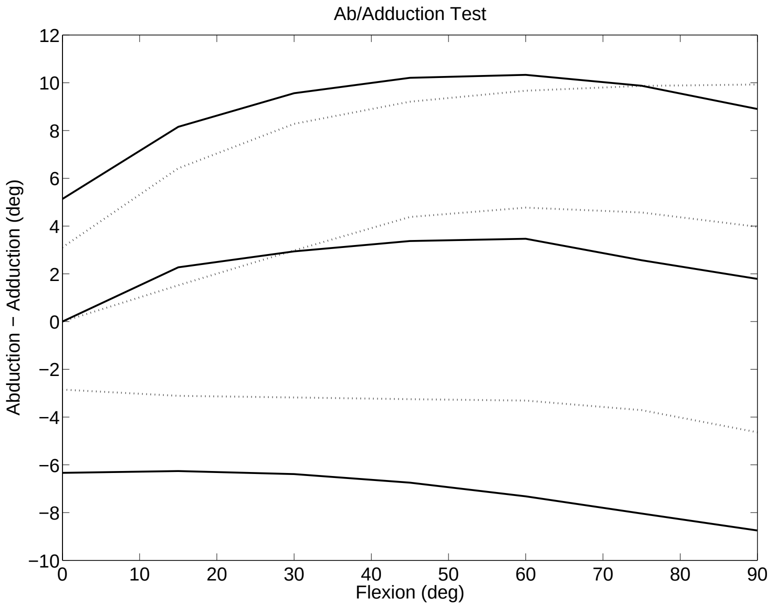

Figure 3.15: Ab/adduction angular displacements of $\mathscr{S}_t$ with respect to $\mathscr{S}_f$. Results of the stiffness model (solid) compared with the experimental data of the reference paper (dot).

(solid lines) components of the position and rotation of $\mathscr{S}_t$ in $\mathscr{S}_f$ during the respective clinical tests: the two pairs of curves are related to conditions with opposite loading directions. Middle curves in Figures 3.14 and 3.15 are the intra/extra and ab/adduction rotation components of the motion of $\mathscr{S}_t$ in $\mathscr{S}_f$ during the reference passive motion. A more detailed description of the experimental data and, as a consequence, of the results is provided at the end of section 3.1.

The stiffness model replicates the experimental results well, especially considering that the reference motions and the anatomical parameters of some structures are taken from the literature and were not recorded during the experimental session. The stiffness of the model is tendentially lower than that reported in the reference study. This difference could be imputed to anatomical variability, but it could also be the symptom that the stiffness model does not reproduce the stiffness characteristic of a certain passive structure. As regards this point, it is worth noting that the capsular structures are not modelled, because of the lack of experimental data, while the experimental motions of [12] refer to intact knees. As a partial confirmation of this point, the optimized values of the stiffness parameters are higher than those in the literature on average: the missing capsula is compensated in the optimization process by a higher stiffness of the other passive structures. The same results were obtained also in [4].

The optimized values of L_{0j} lengths are very close to their first estimates. If these parameters are not optimized, i.e. they are fixed to their first estimate L_{0j}^{min}, the computational time of the identification process becomes considerably lower than that of the full optimization, and the results are paradoxically better than the previous ones: the genetic algorithm can handle the optimization problem better and can find the minimum of the objective function more easily. If L_{0j} lengths are fixed to smaller values than L_{0j}^{min} (thus violating the second rule of the sequential approach), slightly better results for the stiffness model are found until $L_{0j} = 0.99\ L_{0j}^{min}$. This could be a consequence of experimental errors and of anatomical variability. If L_{0j} lengths are fixed to even lower values, the results dramatically worsen. This aspect is a further confirmation of the accuracy of the geometrical and kinematical assumptions which brought to the definition of the proposed knee models and, more in general, of the sequential approach.

Chapter 4

Conclusion

Mathematical models of the knee joint are important tools which have both theoretical and practical applications. They are used by researchers to fully understand the stabilizing role of the components of the joint, by engineers as an aid for prosthetic design, by surgeons during the planning of an operation or during the operation itself, and last, but not least, by orthopedists for diagnosis and rehabilitation purposes.

The principal aims of knee models are to reproduce the restraining function of each structure of the joint and to replicate the relative motion of the bones which constitute the joint itself. It is clear that the first point is functional to the second one. However, the standard procedures for the dynamic modelling of the knee tend to be more focused on the second aspect: the motion of the joint is correctly replicated, but the stabilizing role of the articular components is somehow lost.

A first contribution of this dissertation is the definition of a novel approach — called sequential approach — for the dynamic modelling of the knee. The procedure makes it possible to develop more and more sophisticated models of the joint by a succession of steps, starting from a first simple model of its passive motion. The fundamental characteristic of the proposed procedure is that the results obtained at each step do not worsen those already obtained at previous steps, thus preserving the restraining function of the knee structures.

The models which stem from the first two steps of the sequential approach are then presented. The result of the first step is a model of the passive motion of the knee, comprehensive of the patello-femoral joint. Kinematical and anatomical considerations lead to define a one dof rigid link mechanism, whose members represent determinate components of the joint. The result of the second step is a stiffness model of the knee. This model is obtained from the first one, by following the rules of the proposed procedure. Both models have been identified from experimental data by means of an optimization procedure. The simulated motions of the models then have been compared to the experimental ones.

Both models accurately reproduce the motion of the joint under the corresponding loading conditions. Moreover, the sequential approach makes sure the results obtained at the first step are not worsened at the second step: the stiffness model can also reproduce the passive motion of the knee with the same accuracy than the previous simpler model.

In conclusion, the procedure proved to be successful and thus promising for the definition of more complex models which could also involve the effect of muscular forces.

Bibliography

[1] C. Belvedere, F. Catani, A. Ensini, J. L. Moctezuma de la Barrera, and A. Leardini. Patellar tracking during total knee arthroplasty: an in vitro feasibility study. *Knee Surgery, Sports Traumatology, Arthroscopy*, 15:985–993.

[2] M.Z. Bendjaballah, A. Shirazi-Adl, and D.J. Zukor. Biomechanical response of the passive human knee joint under anterior-posterior forces. *Clinical Biomechanics*, 13(8):625–633, 1998.

[3] L. Blankevoort and R. Huiskes. Ligament-bone interaction in a three-dimensional model of the knee. *ASME Journal of Biomechanical Engineering*, 113(3):263–269, 1991.

[4] L. Blankevoort and R. Huiskes. Validation of a three-dimensional model of the knee. *Journal of Biomechanics*, 29(7):955–961, 1996.

[5] L. Blankevoort, J.H. Kuiper, R. Huiskes, and H.J. Grootenboer. Articular contact in a three-dimensional model of the knee. *Journal of Biomechanics*, 24(11):1019–1031, 1991.

[6] A. Erdemir, S. McLean, W. Herzog, and A.J. van den Bogert. Model-based estimation of muscle forces exerted during movements. *Clinical Biomechanics*, 22(2):131–154, 2006.

[7] R. Franci and V. Parenti-Castelli. A new tool to investigate the interactions between elastic fibers and rigid bodies. In *Proceedings of IFToMM 2007,* Besançon, France, June 17–21, pages 1–6, 2007.

[8] H.S. Gill and J.J. O'Connor. Biarticulating two-dimensional computer model of the human patellofemoral joint. *Clinical Biomechanics*, 11(2):81–89, 1996.

[9] F.G. Girgis, J.L. Marshall, and A.R.S. Al Monajem. The cruciate ligaments of the knee joint. anatomical, functional and experimental analysis. *Clinical Orthopaedics and Related Research*, 106:216–231, 1975.

[10] J.D. Goodfellows and J.J. O'Connor. The mechanics of the knee and prosthesis design. *Journal of Bone Joint Surgery [Br]*, 60-B:358–369, 1978.

[11] E.S. Grood and M.S. Hefzy. An analytical technique for modeling knee joint stiffness — Part I: Ligamentous forces. *ASME Journal of Biomechanical Engineering*, 104(4):330–337, 1982.

[12] E.S. Grood, S.F. Stowers, and F.R. Noyes. Limits of movement in the human knee. *The Journal of Bone and Joint Surgery*, 70-A(1):88–97, 1988.

[13] E.S. Grood and W.J. Suntay. A joint coordinate system for the clinical description of three-dimensional motions: application to the knee. *ASME Journal of Biomechanical Engineering*, 105:136–144, 1983.

[14] C.D. Harner, G. Hyun Baek, T.M. Vogrin, G.J. Carlin, S. Kashiwaguchi, and S.L-Y. Woo. Quantitative analysis of human cruciate ligament insertions. *Arthroscopy: The Journal of Arthroscopic and Related Surgery*, 15(7):741–749, 1999.

[15] J. Heegaard, P.F. Leyvraz, A. Curnier, L. Rakotomanana, and R. Huiskes. The biomechanics of the human patella during passive knee flexion. *Journal of Biomechanics*, 28(11):1265–1279, 1995.

[16] M.S. Hefzy and T.D.V. Cooke. Review of knee models: 1996 update. *Applied Mechanics Reviews*, 49(10-2):187–193, 1996.

[17] M.S. Hefzy and H. Yang. Three-dimensional anatomical model of the human patello-femoral joint to determine patello-femoral motions and contact characteristics. *Journal of Biomedical Engineering*, 15:289–302, 1993.

[18] S. Hirokawa and R. Tsurunob. Three-dimensional deformation and stress distribution in an analytical/computational model of the anterior cruciate ligament. *Journal of Biomechanics*, 33(9):1069–1077, 2000.

[19] R. Di Gregorio and V. Parenti-Castelli. A spatial mechanism with higher pairs for modelling the human knee joint. *ASME Journal of Biomechanical Engineering*, 125(2):232–237, 2003.

[20] R.F. La Prade, C. Muench, F. Wentorf, and J.L. Lewis. The effect of injury to the posterolateral structures of the knee on force in a posterior cruciate ligament graft. a biomechanical study. *The American Journal of Sports Medicine*, 30:233–238, 2002.

[21] A. Menschik. Mechanik des kniegelenks, teil 1. Zeitschrift für Orthopädie, 112:481–495, 1974.

[22] J.-P. Merlet. Kinematics and synthesis of cams-coupled parallel robots. In *Proceedings of CK2005,* Cassino, Italy, May 4–6, pages 1–12, 2005.

[23] K.E. Moglo and A. Shirazi-Adl. On the coupling between anterior and posterior cruciate ligaments, and knee joint response under anterior femoral drawer

in flexion: a finite element study. *Clinical Biomechanics*, 18(8):751–759, 2003.

[24] T.J.A. Mommersteeg, L. Blankevoort, R. Huiskes, J.G.M. Kooloos, and J.M.G. Kauer. Characterization of the mechanical behavior of human knee ligaments: a numerical-experimental approach. *Journal of Biomechanics*, 29(2):151–160, 1996.

[25] T.J.A. Mommersteeg, R. Huiskes, L. Blankevoort, J.G.M. Kooloos, and J.M.G. Kauer. An inverse dynamics modeling approach to determine the restraining function of human knee ligament bundles. *Journal of Biomechanics*, 30(2):139–146, 1997.

[26] T.J.A. Mommersteeg, R. Huiskes, L. Blankevoort, J.G.M. Kooloos, J.M.G. Kauer, and P.G.M. Maathuis. A global verification study of a quasi-static knee model with multi-bundle ligaments. *Journal of Biomechanics*, 29(12):1659–1664, 1996.

[27] J.J. O'Connor, T.L. Shercliff, E. Biden, and J.W. Goodfellow. The geometry of the knee in the sagittal plane. *Proceedings of the Institution of Mechanical Engineers. Part H, Journal of Engineering in Medicine*, 203(4):223–233, 1989.

[28] A. Ottoboni, V. Parenti-Castelli, and A. Leardini. On the limits of the articular surface approximation of the human knee passive motion models. In *Proceedings of AIMeTA 2005,* Firenze, Italy, September 11–15, pages 1–12, 2005.

[29] A. Ottoboni, N. Sancisi, V. Parenti-Castelli, C. Belvedere, and A. Leardini. Equivalent spatial mechanisms for modelling passive motion of the human knee. In *Proceedings of ISB2007,* Taipei, Taiwan, July 1–5, page 1, 2007.

[30] M.G. Pandy. Computer modeling and simulation of human movement. *Annual Review of Biomedical Engineering*, 3:245–273, 2001.

[31] M.G. Pandy, K. Sasaki, and S. Kim. A three-dimensional musculoskeletal model of the human knee joint. part 1: theoretical construction. *Computer Methods in Biomechanics and Biomedical Engineering*, 1:87–108, 1997.

[32] V. Parenti-Castelli, A. Leardini, R. Di Gregorio, and J.J. O'Connor. On the modeling of passive motion of the human knee joint by means of equivalent planar and spatial parallel mechanisms. *Autonomous Robots*, 125(2):219–232, 2003.

[33] V. Parenti-Castelli and R. Di Gregorio. Parallel mechanisms applied to the human knee passive motion simulation. In J. Lenarcic and M. Stanisic, editors, *Advances in Robot Kinematics*. Kluwer Academic, 2000.

[34] Primal Pictures. *Primal 3D Interactive series: Knee*. Primal Pictures Ltd, 2003.

[35] E.A. Rahman and M.S. Hefzy. A two-dimensional dynamic anatomical model of the human knee joint. *ASME Journal of Biomechanical Engineering*, 115:357–365, 1993.

[36] N. Sakai, Z.-P. Luo Z.-P., J.A. Rand, and K.-N. An. Quadriceps forces and patellar motion in the anatomical model of the patellofemoral joint. *The Knee*, 3(1):1–7, 1996.

[37] N. Sancisi and V. Parenti-Castelli. A 1-dof parallel spherical wrist for the modelling of the knee passive motion. In *Proceedings of IFToMM 2007,* Besançon, France, June 17–21, pages 1–6, 2007.

[38] N. Sancisi and V. Parenti-Castelli. A new 3d kinematic model of the patello-femoral joint during knee passive motion. In *Proceedings of AIMeTA 2007,* Brescia, Italy, September 11–14, pages 1–12, 2007.

[39] N. Sancisi and V. Parenti-Castelli. On the synthesis of a 5-5 parallel mechanism reproducing the knee passive motion by means of the Burmester theory. In *Proceedings of CMSM 2007,* Monastir, Tunisia, March 19–21, pages 1–6, 2007.

[40] N. Sancisi, V. Parenti-Castelli, and A. Leardini. A Matlab procedure for the solution of non-linearly constrained optimization problems. In *Proceedings of RAAD05,* Bucharest, Romania, May 26–28, pages 1–6, 2005.

[41] K.B. Shelburne and M.G. Pandy. A dynamic model of the knee and lower limb for simulating rising movements. *Computer Methods in Biomechanics and Biomedical Engineering*, 5(2):149–159, 2002.

[42] K.B. Shelburne, M.R. Torry, and M.G. Pandy. Muscle, ligament, and joint-contact forces at the knee during walking. *Medicine and Science in Sports and Exercise*, 37(11):1948–1956, 2005.

[43] S. Sudasna, K. Harnsiriwattanagit, and C. May. Ligamentous structures of the posterolateral aspect of the knee. *Bulletin of the Hospital for Joint Diseases Orthopaedic Institute*, 50(1):35–40, 1990.

[44] D.R. Wilson, J.D. Feikes, and J.J. OConnor. Ligaments and articular contact guide passive knee flexion. *Journal of Biomechanics*, 31(12):1127–1136, 1998.

[45] D.R. Wilson and J.J. O'Connor. A three-dimensional geometric model of the knee for the study of joint forces in gait. *Gait and Posture*, 5:108–115, 1997.

[46] S.L.-Y. Woo, S.D. Abramowitch, R. Kilger, and R. Liang. Biomechanics of knee ligaments: injury, healing, and repair. *Journal of Biomechanics*, 39(1):1–20, 2006.